AD/A-003 666

LASER WINDOW SURFACE FINISHING AND COATING TECHNOLOGY

Morris Braunstein

Hughes Research Laboratories

Prepared for:

Advanced Research Projects Agency
Air Force Cambridge Research Laboratories

August 1974

DISTRIBUTED BY:

NTIS

National Technical Information Service
U. S. DEPARTMENT OF COMMERCE

UNCLASSIFIED

SECURITY CLASSIFICATION OF THIS PAGE (When Date Entered)

REPORT DOCUMENTATION PAGE		READ INSTRUCTIONS BEFORE COMPLETING FORM
1. REPORT NUMBER AFCRL-TR-74-0425	2. GOVT ACCESSION NO.	3. RECIPIENT'S CATALOG NUMBER AD/A-003666
4. TITLE (and Subtitle) LASER WINDOW SURFACE FINISHING AND COATING TECHNOLOGY		5. TYPE OF REPORT & PERIOD COVERED Semiannual Tech.Rpt. 2 6. PERFORMING ORG. REPORT NUMBER
7. AUTHOR(s) Morris Braunstein		8. CONTRACT OR GRANT NUMBER(s) F19628-73-C-0243
9. PERFORMING ORGANIZATION NAME AND ADDRESS Hughes Research Laboratories 3011 Malibu Canyon Road Malibu, CA 90265		10. PROGRAM ELEMENT, PROJECT, TASK AREA & WORK UNIT NUMBERS 61102E, 2415, T&WU n/a BPAC n/a
11. CONTROLLING OFFICE NAME AND ADDRESS Air Force Cambridge Research Laboratories Hanscom AFB, Massachusetts 01731 Contract Monitor: Dr. Harold Rosen/LQO		12. REPORT DATE August 1974 13. NUMBER OF PAGES 59
14. MONITORING AGENCY NAME & ADDRESS (if different from Controlling Office)		15. SECURITY CLASS. (of this report) Unclassified 15a. DECLASSIFICATION DOWNGRADING SCHEDULE

16. DISTRIBUTION STATEMENT (of this Report)

Approved for public release; distribution unlimited.

17. DISTRIBUTION STATEMENT (of the abstract entered in Block 20, if different from Report)

18. SUPPLEMENTARY NOTES

This research was sponsored by Defense Advanced Research Projects Agency, ARPA Order No. 2415.

19. KEY WORDS (Continue on reverse side if necessary and identify by block number)

Laser Windows, Surface Finishing, Thin Films, Antireflection Coatings, 10.6 μm, 5 μm, Laser Damage Studies, Surface Characterization, Optical Evaluation, Potassium Chloride, Zinc Selenide, Alloys of Halides, Calcium Fluoride

20. ABSTRACT (Continue on reverse side if necessary and identify by block number)

We report on the objectives and the progress achieved in a program to study the surface finishing and coating of laser windows. The program covers six areas of study: surface finishing, surface characterization, coating techniques, optical evaluation, chemical analysis, and laser window damage studies. Potassium chloride surfaces have been produded on reactive atmosphere processed (RAP) KCl using HCl etching which show an order of magnitude improvement in KCl surface damage resistance.

DD FORM 1 JAN 73 1473 EDITION OF 1 NOV 65 IS OBSOLETE

UNCLASSIFIED

SECURITY CLASSIFICATION OF THIS PAGE (When Date Entered)

Reproduced by
NATIONAL TECHNICAL
INFORMATION SERVICE
U S Department of Commerce
Springfield VA 22151

Surface damage level approaches the bulk level in some KCl samples. KCl surface damage levels >1500 J/cm^2 for 600 ns pulses have been obtained with bulk damage levels >3000 J/cm^2 at the same pulse duration. An inverse dependence of 10.6 μm optical absorption on film deposition rate is reported for germanium films, β of ≈10/cm^{-1} is reported for the best films. Ion beam sputtering of ThF_4 using pure argon ion beams results in films deficient in fluorine having high optical absorption at 10.6 μm. Reactive sputtering in argon-fluorine gas mixtures may be required for producing stoichiometric fluoride films. Rutherford backscattering for chemical analysis of films and window surface structure promises to be a new powerful technique for such studies, using moderate beam energies of 180 KeV H^+ and 280 KeV H^{++}.

ARPA Order No.	2415
Program Code No.	3D10
Contract No.	F19628-73-C-0243
Contractor	Hughes Research Laboratories
Effective Date of Contract	1 May 1973
Contract Expiration Date	31 October 1974
Principal Investigator	Morris Braunstein (213) 456-6411, ext. 404
AFCRL Project Scientist	Dr. Harold Posen (617) 861-3532

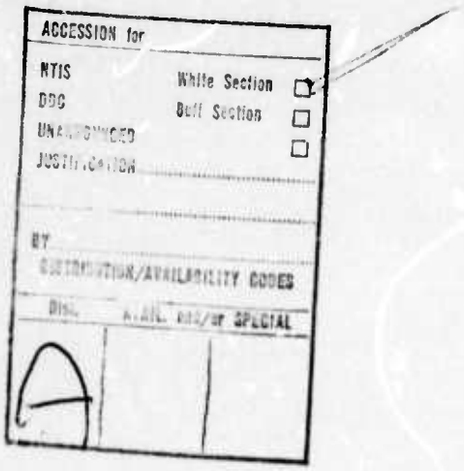

Qualified requestors may obtain additional copies from the Defense Documentation Center. All others should apply to the National Technical Information Service.

TABLE OF CONTENTS

LIST OF ILLUSTRATIONS

Preceding page blank

I. INTRODUCTION

Hughes Research Laboratories (HRL) is engaged in a broad program to develop laser window surface finishing and coating technology. Extensive investigations are under way in many laboratories throughout the country, as well as at HRL, to develop window materials that have both the low optical absorption and the high tensile yield stress necessary to satisfy system applications. Two classes of materials — the wide bandgap semiconductors and the alkali halides — have received major emphasis in these investigations. The goal of our program at HRL is to investigate the surface characteristics and the optical coatings applied to laser windows in order to develop optimized finishing and coating procedures so that the laser damage thresholds of the coatings and surfaces approximate as closely as possible the damage thresholds of the bulk window materials. At present, serious limitation to window performance characteristics can exist because as the laser pulse duration is shortened and the peak power densities rise, the low damage threshold of some of the presently available coatings and surfaces can cause damage to occur below the bulk material damage threshold. This lowered damage threshold caused by the presence of pores and microcracks which can be present in window surfaces and coatings was the subject of a report by Bloembergen and Stickley,[1] which focused early attention on the importance of launching a research effort on surfaces and coatings to provide improvements in the state of the art.

This report presents results we have achieved for the period 1 November 1973 through 30 April 1974. The program places emphasis on studies for 10.6 μm applications; however, studies at 5.3 μm are also performed where required.

---

[1] N. Bloembergen and C.M. Stickley, Report of the ARPA 1972 Materials Research Council, E.E. Hucke, Editor, University of Michigan (1972).

Preceding page blank

II. TECHNICAL DISCUSSION

A. Coating Techniques

During the course of our program it is our objective to prepare antireflection (AR) film coatings for candidate infrared laser window materials by three film preparation techniques: ultrahigh vacuum deposition, ion beam sputtering, and chemical vapor deposition. Using these techniques the films are compared in an effort to determine an optimized method of preparation for use of the films in high energy laser window applications.

1. Ultrahigh Vacuum Film Deposition

a. Germanium Films — The work on germanium film preparation which was reported in preliminary form in Semiannual Technical Report 1 has been completed. The inverse dependence of 10.6 μm absorption on film deposition rate was confirmed. Correlations were found between the deposition rate, the impurity content, and physical structure of the films which appear to explain the results.

Figure 1 summarizes the germanium film absorption versus deposition rate results. The points which fall on the dashed curve are for films of more than a few hundred angstroms in thickness. These points clearly show the inverse dependence of 10.6 μm absorption on deposition rate. Other deposition parameters, such as substrate temperature and system pressure during deposition, were found not to affect the absorption results within the ranges studied (pressure: 1.5×10^{-7} - 2.5×10^{-9} Torr; temperature 27 to 150°C). The two points which are labled "90 Å film" in Fig. 1 are indicative of an excess absorption in thin layers which is probably concentrated at the film-substrate interface. This high apparent absorption coefficient in thin layers is a result of assuming a uniform absorption coefficient throughout the layer and thereby neglecting the possibility of any surface effects. For the thicker layers the error introduced is small since the surface absorption is a small percentage of the total absorption. It

Preceding page blank

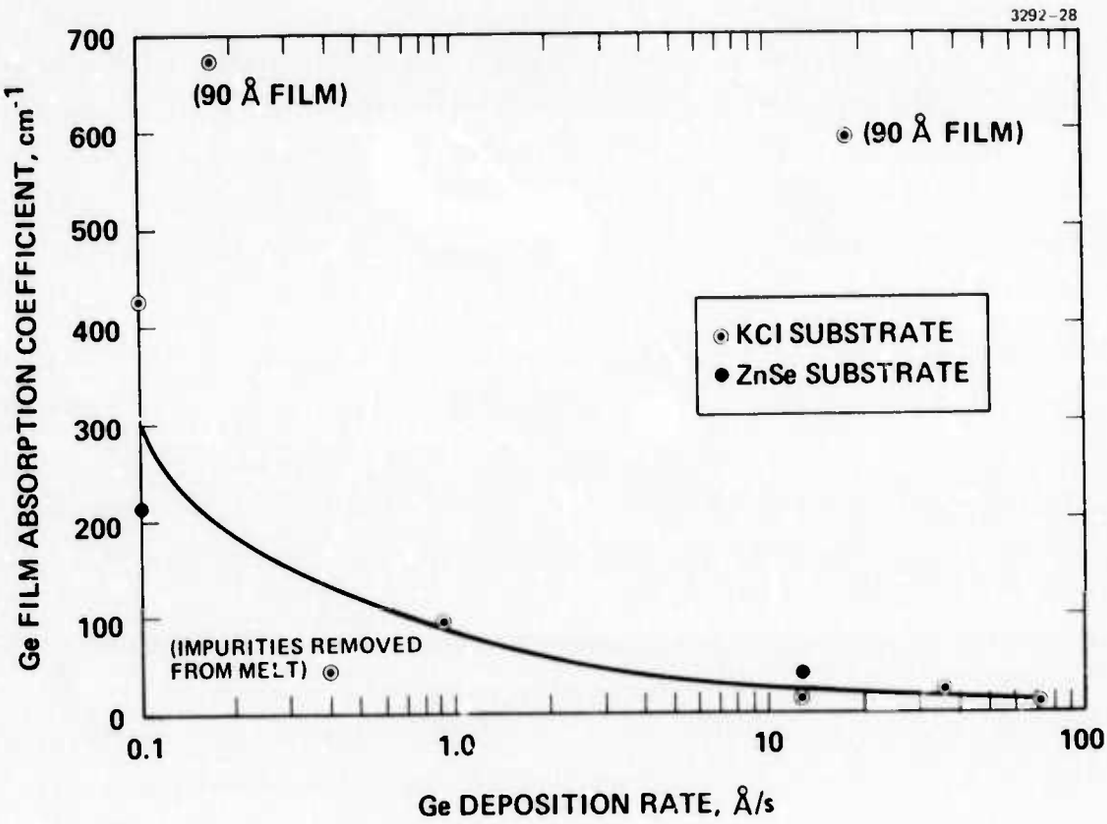

Fig. 1. 10.6 μm absorption versus deposition rate for UHV germanium films.

was believed at first that the controlling parameter in the absorption data was the amount of potassium and chlorine interdiffusion between the germanium film and the KCl substrates (see Semiannual Technical Report 1.). This potential explanation was weakened by finding the same rate dependence of absorption on ZnSe substrates as on KCl. It was subsequently found that the interdiffusion was essentially eliminated when the substrate temperature during deposition was reduced from about 150°C to 80°C or less. The rate dependence of absorption did not change at this point; therefore, other explanations were sought. Heavy metal impurities which were detected in the germanium films by Rutherford backscattering were found to be correlated with gold and barium found by electron microprobe analysis in the tip of the germanium source material.

A germanium film prepared after removal of these impurities from the germanium melt had a greatly reduced heavy metal content and had low absorption compared with previous films. A partial explanation of the rate dependence of absorption is provided by these observations. The impurities in the germanium source material were concentrated in the last-to-freeze portion of the conical-shaped melt that develops when the e-gun evaporator is turned off after a run. In subsequent runs at low rates only this tip of the germanium material is melted by the e-gun, and, therefore, the impurity content of the evaporating material is probably high. When a run is made at high deposition rate the entire germanium charge is melted, the impurities are dissolved in a large amount of germanium, and the impurity content of the evaporating material is probably low. The amount of gold which was present at the melt tip is consistent with the gold concentration which would have been used to dope the germanium for high resistivity. The vacuum melting and slow cooling which we have subjected the material to has probably resulted in a zone refining action (It should be pointed out that the Ge source material was purchased with the condition that it be vacuum zone refined material of 99.999% purity, or better, with respect to metals.) The heavy metal

impurities cannot be responsible for the entire rate dependence of the absorption for a number of reasons. Even after removal of most of the heavy metal contamination there is still an excess absorption of a factor of four for films prepared at low rates over those prepared at high rates. A further confirmation of this excess is the fact that germanium films sputtered at 0.5 Å/s were found to have absorptions in the neighborhood of 10 cm^{-1}. Therefore, a study of the physical structure of germanium films on KCl and ZnSe substrates was initiated.

X-ray diffractometer scans taken on films on KCl and ZnSe prepared at both high and low rates showed only a broad low angle continuum from the germanium films. This is usually taken to be indicative of an amorphous structure, but is not conclusive for thin films. Reflection electron diffraction observations were done next on the same four samples. The high rate films showed a diffuse low angle scattering, which is again indicative of amorphous structure. In this experiment the low rate films showed well developed debye rings indicative of polycrystalline structure with no preferred orientation. Finally, the films on the KCl substrates were floated free by immersion in water and mounted on copper grids for examination by transmission electron diffraction. The low rate film was found to consist of randomly oriented crystallites with a size equal to or less than the 100 Å electron beam diameter. The high rate film was too thick to transmit the electron beam and, therefore, could not be studied by this method. It is probable, however, that it would have been found to be truly amorphous. These observations provide the probable reason for the remainder of the excess 10.6 μm absorption in low rate films as an effect of departure from amorphous structure. They support the conclusions as to structural effects on the infrared absorption of germanium films arrived at by T. Donovan (NWC-China Lake) by indirect means.

b. $\underline{ThF_4\ Films}$ — At the conclusion of the work on ultrahigh vacuum deposition of germanium, attention was turned to ThF_4. The germanium work was useful in learning to deposit and

monitor films in the UHV system and in evaluating the usefulness of the various physical and chemical analytical tools at our disposal. However, it is not expected that germanium will be a usable film material for most high energy laser applications nor is it clear that UHV deposition provides any advantage over conventional vacuum for it. The situation is expected to be different for ThF_4. It is the best available low index material for 10.6 μm use which is not water soluble. Furthermore, in the UHV environment the major residual gas after bakeout is hydrogen rather than water as in conventional systems. For a fluoride material whose infrared absorption is strongly affected by oxygen and OH^- content the environment in the UHV system should lead to reduced absorption in the films.

In the initial ThF_4 depositions the water residual was relatively high and the ThF_4 absorption was similar to that of films prepared in conventional systems. Careful mass spectrographic analysis of residual gases, leak detection, and bakeout testing was initiated in order to be certain that the best possible background conditions are obtained in future depositions.

2. Future Plans

Work on UHV deposition of ThF_4 films will continue until reproducible low absorption films can be prepared. Following this 10.6 μm antireflection coatings will be prepared in the UHV system for absorption measurements and pulsed laser damage testing.

3. Chemical Vapor Deposition (CVD)

The primary objectives of this task include the investigation of chemical vapor deposition and physical vapor deposition (PVD) of chalcogenide materials, especially As_2S_3, for the evaluation of these techniques in producing high quality, protective, antireflective coatings on optical materials such as KCl, ZnSe, and CaF_2.

Early in this period a number of runs were made using an open-tube PVD system (see Fig. 2) in which As_2S_3 was heated in a stream of hot dry nitrogen. Experiments were performed using glass (vitreous silica) substrates as well as cleaved and cut and polished KCl surfaces. The series of experiments indicated that a freshly etched

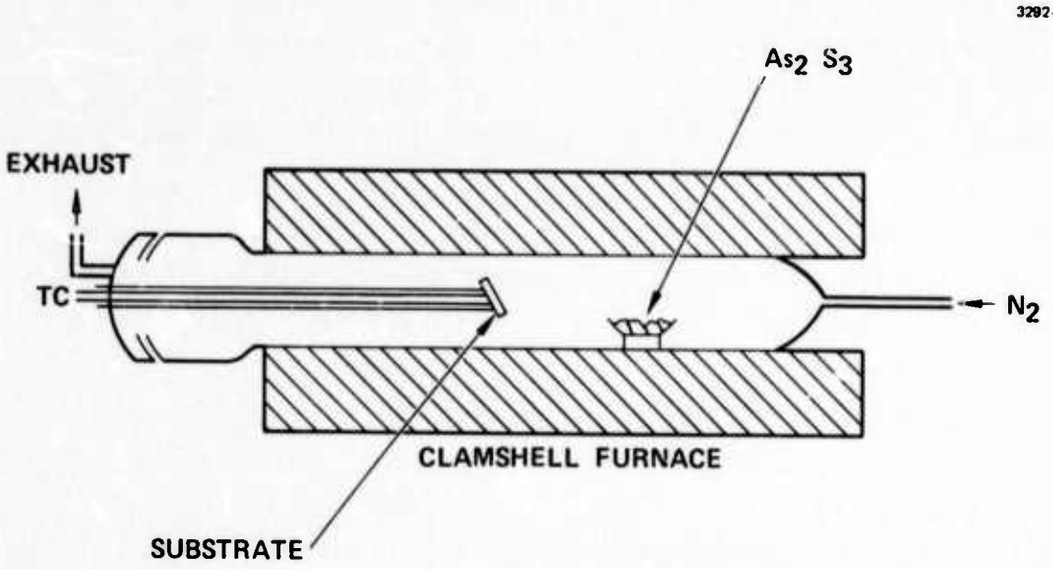

Fig. 2. PVD apparatus.

surface of KCl was necessary in order to get a smooth film. The result of these experiments was the deposition of films of As_2S_2. Because of the difficulties of composition control in this type of apparatus, construction of a chemical vapor deposition (CVD) apparatus got under way.

The CVD apparatus (Figs. 3 and 4) was completed early in 1974. The apparatus is designed for the reaction

$$3H_2S + 2AsCl_3 + H_2 \rightarrow As_2S_3 + 6HCl\uparrow + H_2\uparrow,$$

where H_2 acts as a carrier gas for the As_2Cl_3. Following a few initial runs on glass substrates, freshly HCl-etched KCl has been used. Twelve runs have been made to date.

The following results were obtained:

1. Amorphous films of As_2S_3 have been grown on KCl substrates, typically less than 1 μm thick.

2. Composition of the product being deposited can be controlled by adjusting the flow rates of the H_2S and H_2 (carrier gas for $AsCl_3$).

3. Quality control of the films is strongly dependent on substrate temperature; best films have been grown at temperatures of 150°C but not at lower temperatures.

4. Increased temperature has indicated an epitaxial growth of As_2S_3 on KCl. This is an initial result which is still being evaluated.

The major problems encountered so far have been the growth of crystals of dimorphite (As_4S_3) nucleating within the amorphous As_2S_3 matrix (see Fig. 5(a) and (b)), the crystals appear to grow larger at the expense of surrounding smaller crystals with increased time. Early problems which included room temperature reaction of the constituents have been solved by reactor design. Flow rates in excess of 15 cc/min of H_2S and 70 cc/min of H_2 (which approximately conform to the stoichiometry of the desired product, As_2S_3) have caused streaming in the reaction chamber and subsequent uneven deposition of the

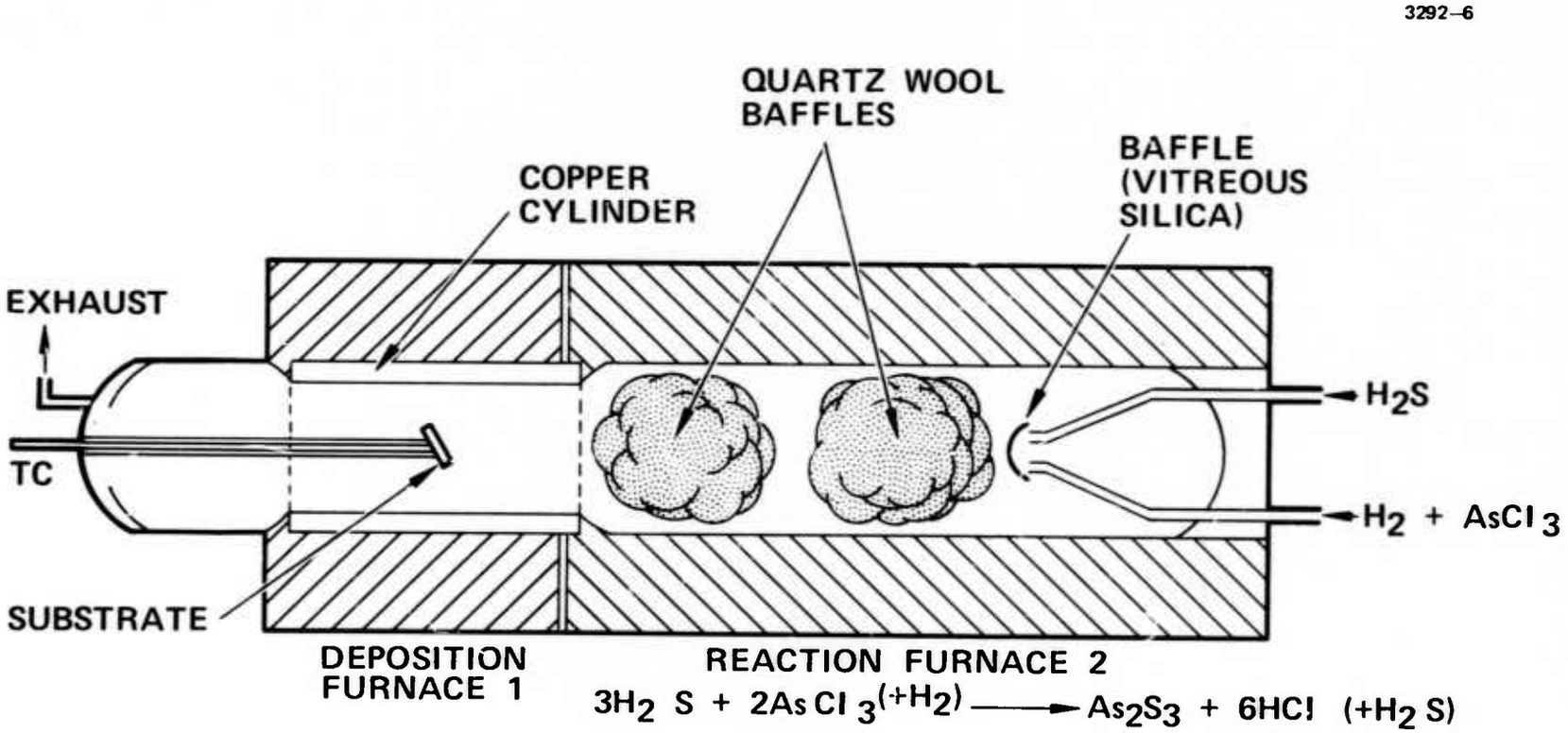

Fig. 3. CVD apparatus.

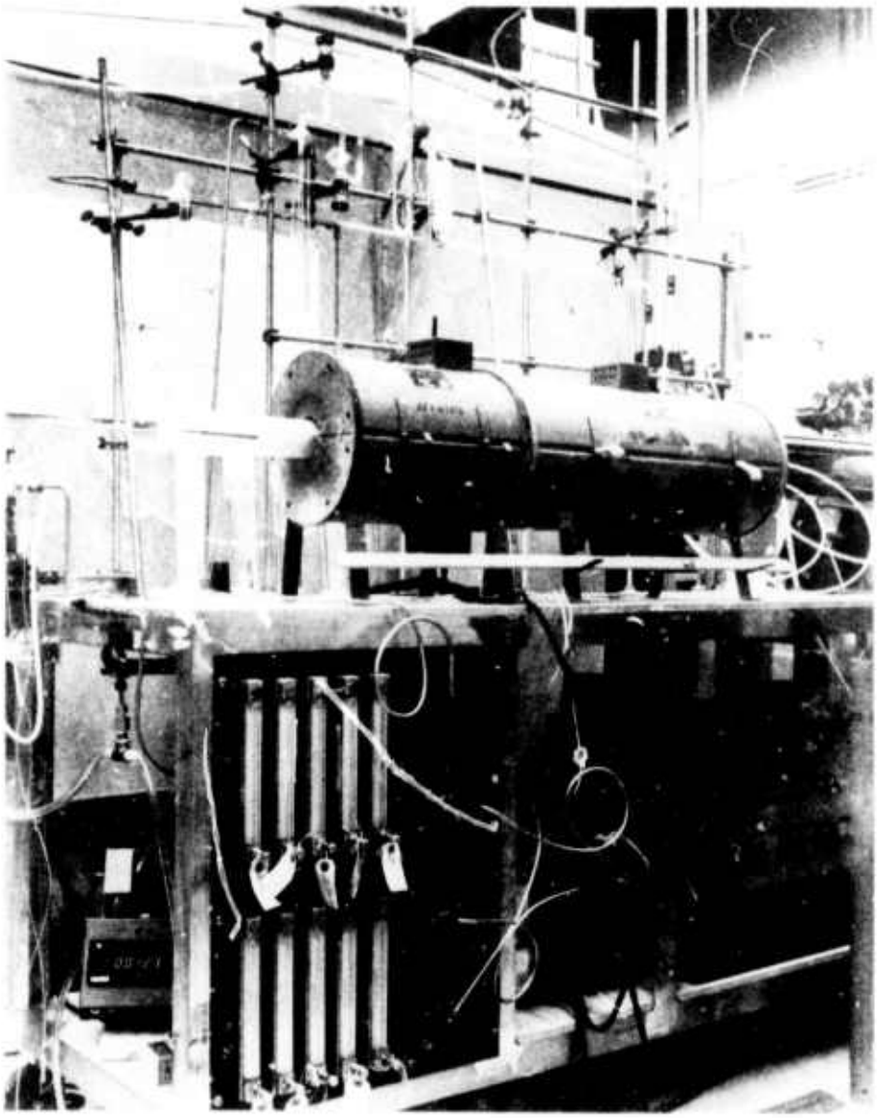

Fig. 4. Chemical vapor deposition of As_2S_3.

350X

Fig. 5(a). Microprobe SEM photograph

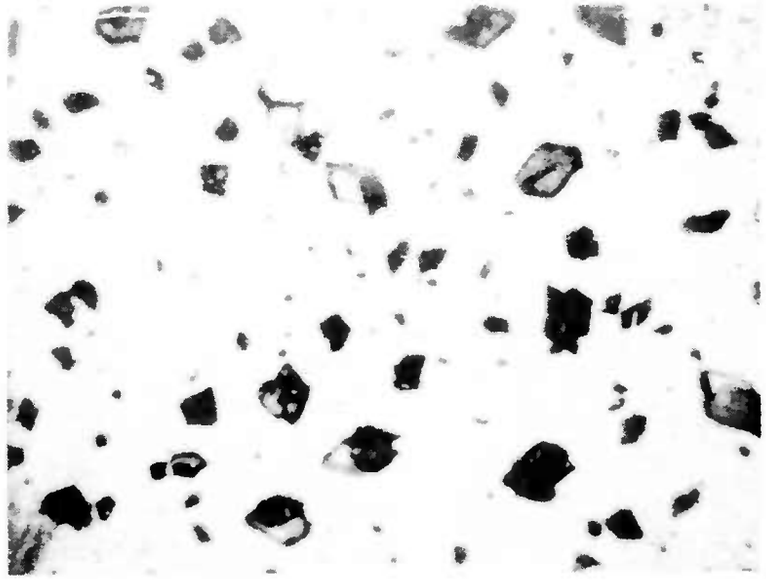

320X

Fig. 5(b). Photomicrograph.

coating. Lower flow rates and the presence of three baffles (two of quartz wool) have eliminated this problem. An additional major problem encountered was the effect of low temperatures in the substrate region wherein major heat flow was by convective forces which resulted in uneven heating of the substrate and hence uneven deposition. The requirement for higher substrate temperatures as well as a thick copper cylinder around the tube in the vicinity of the substrate apparently have solved this problem.

Plans for the future include adjustment of substrate temperature and gas flow rates to improve and control deposition of the desired coating (As_2S_3) of optimum thickness and optical properties. Greater control of coating uniformity both in thickness and in composition appear attainable using the CVD system herein designed. We believe this will produce a protective (no pinholes!) coating for materials like KCl which will require such a coating for any future application as an optical component.

B. Surface and Chemical Characterization

1. Degradation of KCl Surfaces

As discussed in Semiannual Technical Report 1, proton channeling effects can be used to measure the crystalline quality of KCl surfaces. As part of a study to correlate lattice disorder with optical absorption we have used this technique to observe significant degradation of KCl surfaces with time. Backscattered energy spectra of 140 keV protons incident along the <100> channel of a KCl sample soon after etching (within 2 days) and after 2 months storage in a vacuum desiccator are shown in Fig. 6. The sample was a single-crystal platelet (Optovac) which was cleaved along a {100} plane, mechanically polished, etched in HCl for 1 min, and then rinsed in ethanol followed by Freon vapor degreasing. A tungsten filament provided electron flooding during the proton bombardment to prevent charge build-up.

The small peak at the surface (channel 90) of Fig. 6 on the original etched surface is probably caused by a thin oxide layer. The <100> yield just behind this peak is about 5% of the random or

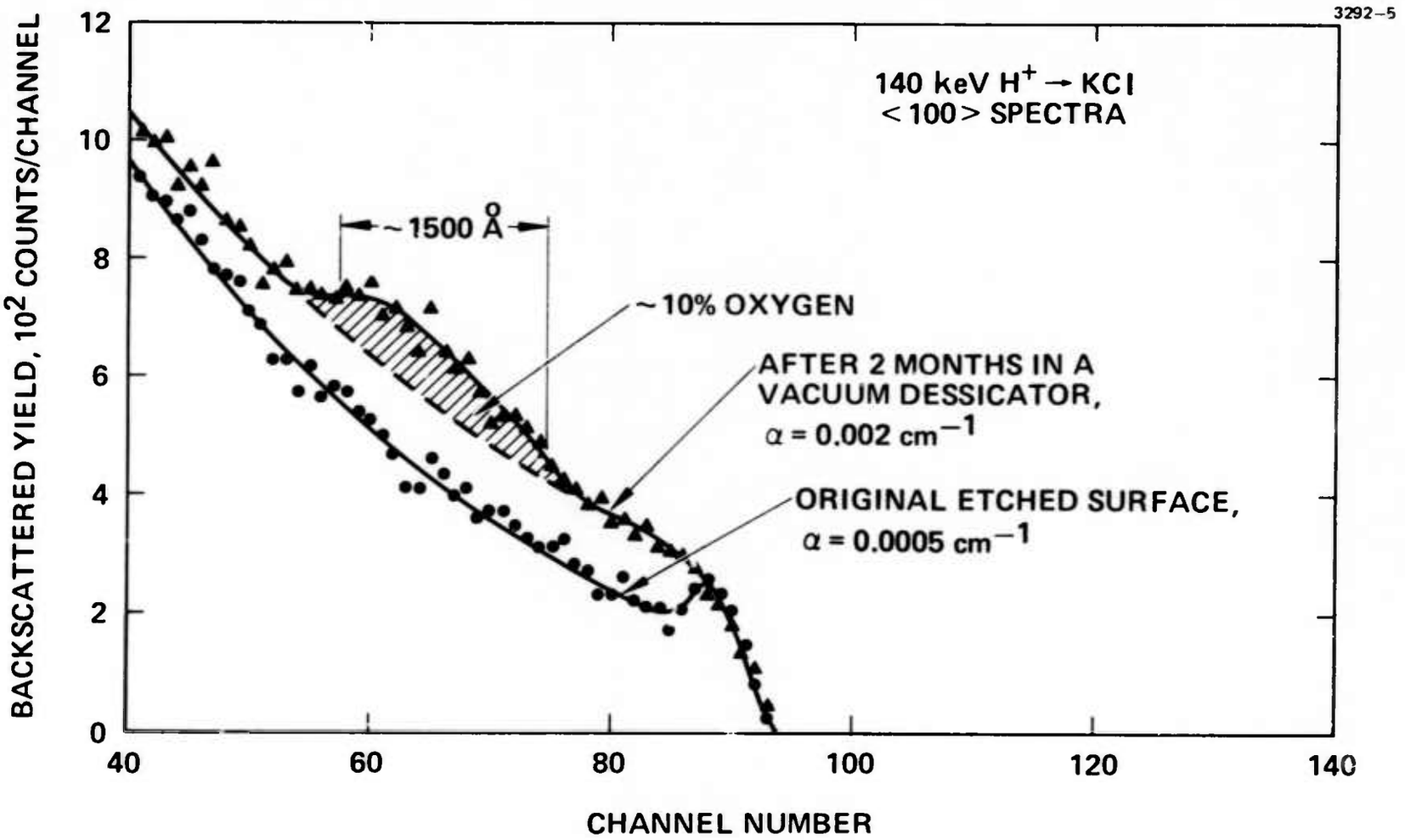

Fig. 6. Backscattered energy spectra of 140 keV protons incident along the 100 channel of KCl after HCl etching and after 2 months' storage in a vacuum desiccator.

nonchanneled yield, a result typical of a good single crystal surface region. However, the <100> spectrum after two months' storage in a vacuum desiccator, which is also shown in Fig. 6, indicates an approximately 50% increase in yield near the surface and a broad peak starting at channel 75. This peak is consistent with the incorporation of about 10% oxygen in a 1500 Å surface layer. The presence of the oxygen apparently causes the increased yield from K and/or Cl atoms near the surface by a distortion of the original lattice. It is also of interest to note that the 10.6 μm absorption coefficient increased from 0.0005 cm^{-1} soon after etching to 0.002 cm^{-1} after two months' storage. Thus there seems to be a definite correlation of increased absorption with chemical and physical degradation of the surface region. Although additional work is needed to better define the reaction rate of KCl surfaces with environmental conditions, the present results suggest that protective coatings of KCl are essential to long-term surface stability even in a relatively H_2O-free environment, i.e., a vacuum desiccator.

2. Germanium Films

It was noted last report period that germanium films deposited on KCl substrates maintained at 150°C during deposition in our ultrahigh vacuum system contained a heavy element, K, and O impurities. The amounts of these impurities were larger at a slow deposition rate (0.6 Å/s) than at a fast deposition rate (27 Å/s). To determine the effect of substrate temperature on the amounts of these impurities, a germanium film was deposited at a low rate (0.17 Å/s) onto a KCl substrate maintained at 30°C. We were particularly interested in determining whether a lower substrate temperature would reduce the amount of K which possibly diffuses into the germanium film from the KCl substrate.

A backscattered energy spectrum using 280 keV He^{++} analysis of this recent germanium film is shown in Fig. 7. The amounts of K and O in the film are less than the measurement sensitivities, ~1% and ~10%, respectively. These results should be contrasted with the 4% K and 20% O observed earlier in the low rate film deposited at 150°C.

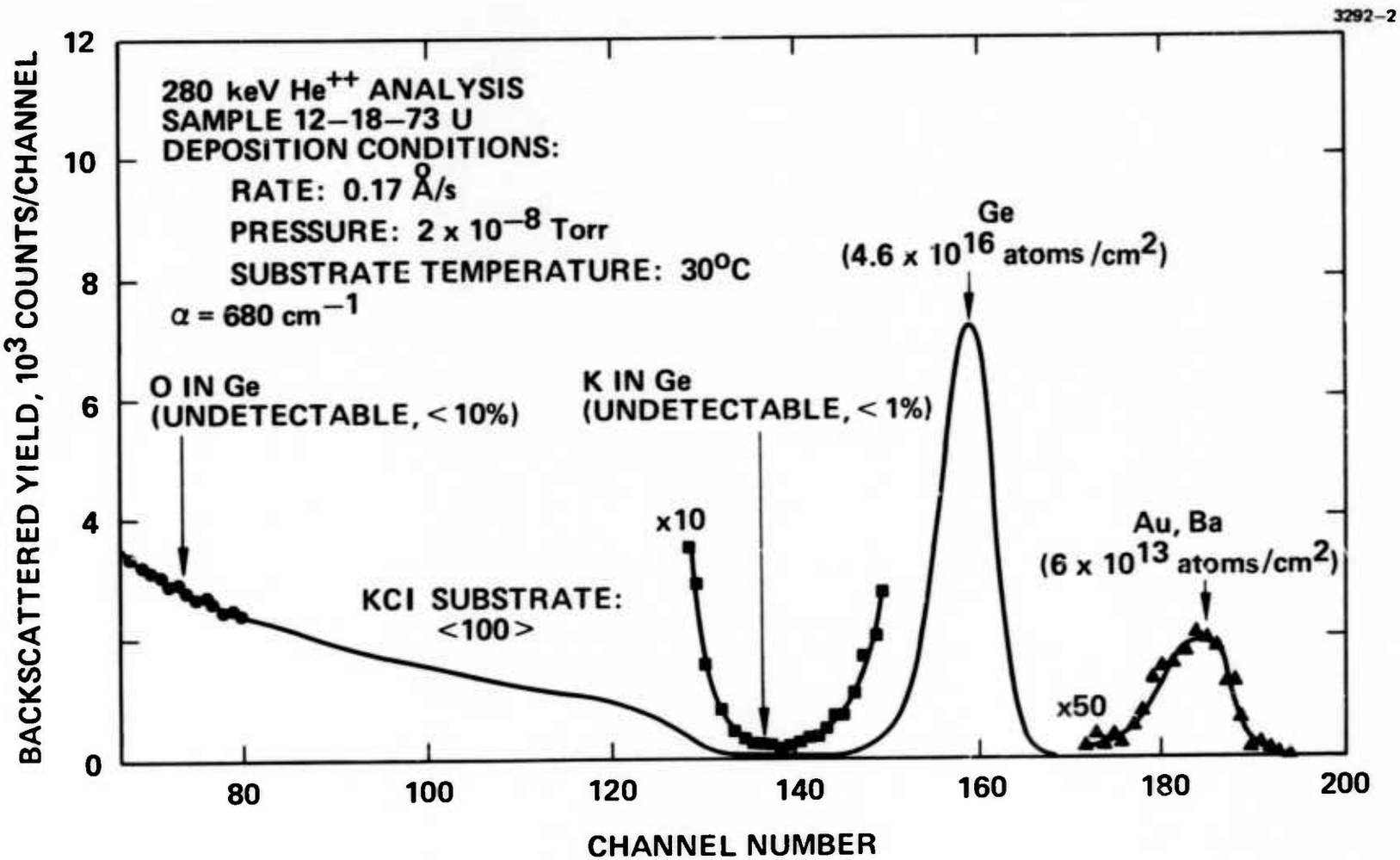

Fig. 7. Backscattered energy spectrum of 280 keV He^{++} incident on a thin germanium film evaporated onto KCl in UHV.

Therefore, a reduction of substrate temperature to 30°C markedly reduces the K and O contents in germanium films on KCl.

However, the heavy impurity peak at channel 185 of Fig. 7 is comparable in amount to the 0.07% observed earlier, and consequently, is unaffected by substrate temperature. Electron microprobe analysis of the surface of the germanium material used for the depositions revealed that trace amounts of gold and barium were located in a small area (100 mil radius) near the tip of the germanium which was locally heated by electron beam bombardment during the depositions.

Thus the heavy element peak of Fig. 7 is attributed to gold and barium. It is postulated that the gold may have been present in the bulk of the germanium and diffused to the tip during e-beam bombardment. To check this point the contaminated tip was lapped away, and another low-rate (0.4 Å/s) germanium film was deposited on KCl. After lapping, microprobe measurements of the germanium source material indicated that the gold and barium had been removed.

A backscattered energy spectrum from this film is shown in Fig. 8. Since the germanium film is much thicker (1350 Å) than that of Fig. 7, the heavy impurity peak is broadened. Nevertheless, the level of the backscattered yield from the heavy impurity near the surface at channel 182 of Fig. 8 is reduced to about 0.5 of the previous level. Microprobe analysis of the tip of the germanium source material after evaporation of the film of Fig. 8 revealed that a trace of barium was again present, but that there was no re-introduction of gold. It seems reasonable to attribute the remaining heavy element concentration (0.05%) in the germanium film of Fig. 8 to barium. Since BaF_2 films were originally deposited in our UHV system, the re-introduction of barium onto the tip of germanium source material and in the deposited film apparently is caused by residual barium contamination of our vacuum chamber. This result points out the difficulty of avoiding cross contamination of different film material deposited in the same system.

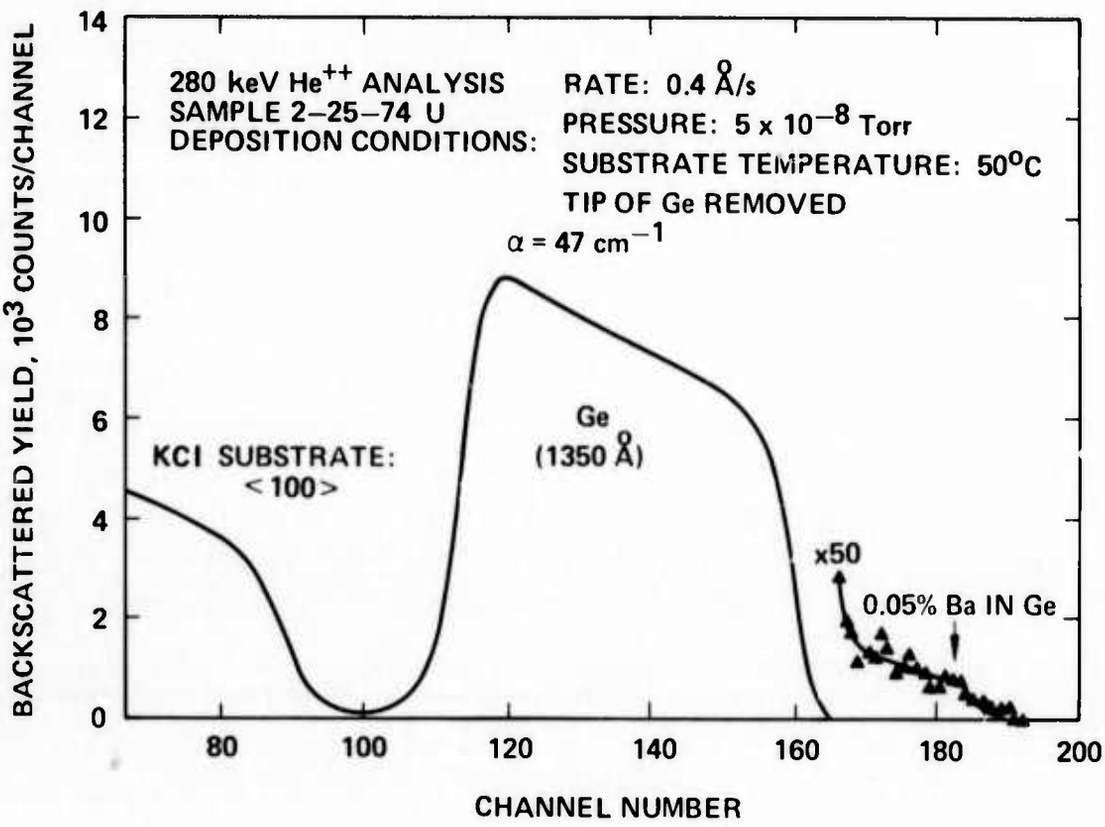

Fig. 8. Backscattered energy spectrum of 280 keV He^{++} incident on a 1350 Å germanium film evaporated onto KCl in UHV after removal of the tip of the germanium source material.

3. Compositions of Fluoride Films

The compositions of several fluoride films were determined during this report period. We were especially interested in comparing the compositions of evaporated and sputter-deposited thorium fluoride. A backscattered energy spectrum of 280 keV He^{++} from an evaporated thorium fluoride film on a carbon substrate is shown in Fig. 9. The amounts of thorium and fluoride in the film are determined from the areas of the peaks corresponding to scattering from thorium and fluoride atoms, respectively, together with the known Rutherford scattering cross sections and are indicated on the figure. The ratio of the number of fluoride atoms to the number of thorium atoms is calculated to be 4.2 ± 5%, the estimated error being caused primarily by uncertainty in the background level of the fluoride peak, the dashed line of Fig. 9. Therefore, this ratio of fluoride to thorium is in agreement with the expected composition of ThF_4. Furthermore, no impurities were detectable.

The results of similar measurements of Ar^+ beam sputter-deposited thorium fluoride and magnesium fluoride together with an electron microprobe analysis of rf plasma sputter-deposited thorium fluoride are summarized in Table I. Also included in the table are the results from the evaporated ThF_4 film discussed above. In all cases the sputter-deposited films were strongly deficient in fluoride. Clearly, normal sputtering procedures are inadequate for the formation of stoichiometric fluoride films. In addition, impurities were detected in the sputter-deposited films as indicated in Table I. It is interesting to note that the source of sodium in the rf plasma-deposited thorium fluoride was traced to the presence of 10% sodium in the sputter target. The Fe(?) and W(?) impurities apparently come from the structure of the sputter ion gun.

C. Optical Evaluation

During the course of our program optical evaluation of windows and coatings is performed using absorption calorimetry, interferometry, polarizing microscopy, optical scattering, and ellipsometry. Most of

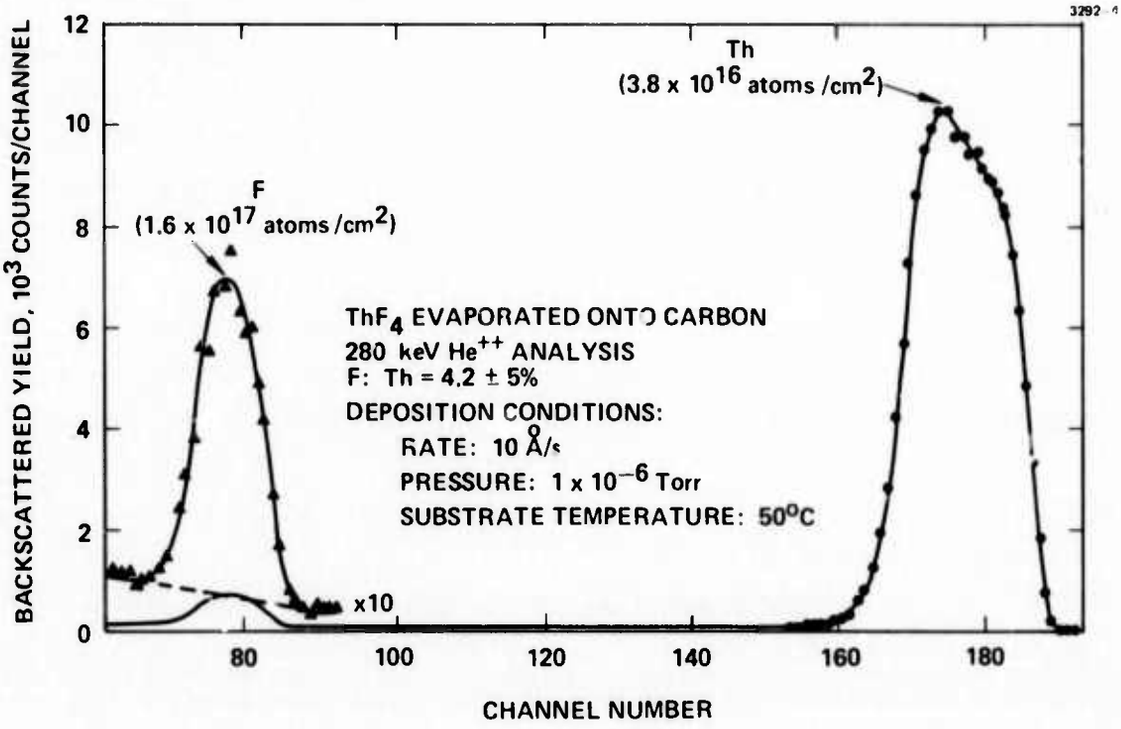

Fig. 9. Backscattered energy spectrum of 280 keV He^{++} incident on a ThF_4 film evaporated onto a carbon substrate.

TABLE I

Compositions of Fluoride Films

Desired Composition	Deposition Technique	Analysis Technique	Actual Composition	Impurities
ThF_4	Evaporation	He^{++}	ThF_4	None detected
ThF_4	Sputtering (rf plasma)	Probe	ThF	4% Na*
ThF_4	Sputtering (Ar^+ beam)	He^{++}	ThF	Ar,Fe(?), W(?)
MgF_2	Sputtering (Ar^+ beam)	He^{++}	MgF	Ar,Fe(?), W(?)

*Electron microprobe analysis of sputter target revealed 10% Na contamination.

T1396

the measurements place emphasis at the 10.6 μm wavelength region; however, 5.3 μm measurements are performed where required.

1. Modulated Light Ellipsometer

To be able to properly design optical coatings and to be able to interpret experimental results it is necessary to have available good data on the optical constants of the materials involved. This is particularly important for film materials, in which the optical properties may depend on preparation conditions, and for new bulk materials, or in cases where surface or interfacial effects are important.

Such information is most expeditiously obtained by the method of ellipsometry, in which polarized light is incident on the sample and the ratio of the amplitude reflectances for light polarized parallel and perpendicular to the plane of incidence is measured. Such an instrument is under construction. The HRL ellipsometer will differ from conventional instruments in several respects, the most significant being the manner in which the data are extracted and the operating wavelength range. In most conventional ellipsometers the optical train consists of light source, polarizer, quarter wave plate, sample, analyzer, and detector. The usual method of operation is to set the polarizer at 45^{o} and then to adjust the quarter wave plate and analyzer (either manually, or under computer control) in order to extinguish the light falling on the detector. This is a very laborious procedure which requires extreme accuracy in the measurement of the final angles of the components in order to extract the desired optical constants.

The HRL instrument will utilize an acousto-optic modulator in place of the quarter wave plate. The polarizer, modulator, and analyzer optic axes can then be left in fixed positions and the data extracted electronically from the signals at the detector at the first and second harmonic of the modulator drive frequency. This method has the advantages of elimination of a tedious measurement procedure, higher sensitivity for the measurement of small absorptions, and the relaxation of the angular accuracy requirements.

A basic modular ellipsometer system with quartz optics has been received from Rudolf Research Corporation, which will operate in the wavelength region from 2000 Å to approximately 8000 Å with a commercial fused quartz modulator and the standard Rudolf photomultiplier detection system. The addition of an InSb detector will permit operation to approximately 4 μm. Also, 10.6 μm operation will be available by using a waveguide laser, ZnSe wire grid polarizer and analyzer, ZnSe modulator, and PbSnTe detector. Most of these components are under construction. The 10.6 μm capability will be unique.

A silicon Schottky barrier detector is on hand to extend the instruments range in the ultraviolet to 2400 Å and in the near infrared to 1.1 μm. A pair of wire grid polarizers have been fabricated on ZnSe, and a 10.6 μm waveguide laser is nearly completed. A ZnSe acousto-optic modulator with quarter wave modulation capability to 4 μm has been operated and a redesigned version is expected to operate to the 10.6 μm region.

During this report period a theoretical analysis of the operation of modulated light ellipsometers was also undertaken. The results of the analysis were used to assist in determination of the specifications for the instrument to be built and allowed a substantial cost saving as a result of relaxation of the usual angular position measurement requirement of ellipsometers. This saving was applied to the optics to allow the purchase of an instrument having a wider-than-normal wavelength range. In addition, an extensive computer program for the analysis of ellipsometer data was obtained from the Nation Bureau of Standards. It has been fully debugged and is now operational on the GE635 computer system although certain minor modifications have not yet been made to permit the handling of the data that will be generated by our modulated light instrument.

D. 10.6 μm Laser Damage

The laser damage effort under the present ARPA-supported program started according to plan in the latter part of November 1973.

A review of our accomplishments to date is best presented by reference to the preprints of two papers in the Appendix of this report. The papers were given at the Symposium on Damage in Laser Materials, Boulder, Colorado May 1974, and will be published in the proceedings of the Symposium.

III. SUMMARY

The work on germanium film preparation which was reported in preliminary form in Semiannual Technical Report 1 is completed. The inverse dependence of 10.6 μm absorption on film deposition rate observed in our initial work is now confirmed. Correlations are found between the deposition rate, the impurity content, and physical structure of the films which appears to explain the variation in the 10.6 μm absorption data. Germanium film absorption continues to be limited to a β of $\approx 10\ cm^{-1}$ for the best films produced. High deposition rates minimize the impurity content in the films and leads to amorphous film structure; both are required for low optical absorption at 10.6 μm. A reduction of the KCl substrate temperatures from 150°C to 30°C markedly reduces the K and O levels in the germanium films on KCl.

Ion sputtering of ThF_4 using pure argon ion beams results in films that are deficient in fluorine and have high optical absorption at 10.6 μm. Reactive ion sputtering in argon-fluorine mixtures for ThF_4 and other fluorides may be required to produce stoichiometric composition films.

A modulated light ellipsometer is under construction for operation out to the 10.6 μm wavelength region, which will provide a unique capability for measurement of the optical constants of films and bulk materials.

Rutherford backscattering and ion channeling analysis at 140 keV and 280 keV continues to be a new powerful tool for investigating surface damage in single crystal surfaces and an equally powerful tool for looking at impurity levels and stoichiometry in films.

Pulsed CO_2 laser damage studies of (HRL) RAP grown KCl show an order of magnitude improvement in KCl surface damage for HCl-etched surfaces. In some KCl samples, KCl surface damage level approaches the bulk damage level. Surface damage levels $> 1500\ J/cm^2$ for 600 ns pulses have been seen with bulk damage levels $> 3000\ J/cm^2$ at the same pulse duration. Previous damage

data in the literature reported as intrinsic level, for KCl, probably were still impurity limited. Our damage, although higher in damage level, may still be impurity limited but appears closer to the intrinsic level.

IV. PLANS FOR NEXT PERIOD

We will continue our work covering the six program elements: surface finishing, surface characterization, coating techniques, optical evaluation, chemical analysis, and 10.6 μm laser damage studies. The work effort will still place emphasis on an integrated research program on the preparation of antireflective coatings for high power infrared laser window materials and the relationship of such preparative procedures to the transmissivity of the coated windows at infrared wavelengths and to the damage mechanisms of such optimally coated windows when subjected to high power infrared laser irradiations. The window materials which are to be investigated will include single and polycrystal KCl, CaF_2, alloy alkali halides, and ZnSe. Selected chalcogenide and fluoride materials, either singly or in multilayer stacks, will be investigated for use as antireflective coatings and the coatings will be evaluated for their infrared transmissivity, adhesion and optical performance under infrared laser irradiation.

APPENDIX

PULSED CO_2 LASER DAMAGE STUDIES OF RAP GROWN KCl

Susan D. Allen, Morris Braunstein, Concettc Giuliano, and Victor Wang

Hughes Research Laboratories
3011 Malibu Canyon Road
Malibu, California 90265

Presented at the Symposium on Damage in Laser Materials, Boulder, Colorado, May 1974. To be published in the Proceedings.

Preceding page blank

Pulsed CO_2 Laser Damage Studies of RAP Grown KCl*

Susan D. Allen, Morris Braunstein, Concetto Giuliano, and Victor Wang

Hughes Research Laboratories
3011 Malibu Canyon Road
Malibu, California 90265

ABSTRACT

Laser damage thresholds in high purity RAP (Reactive Atmosphere Processing) KCl were measured as a function of surface and bulk processing techniques. Single crystal and press forged material was prepared in a "conventionally" polished and HCl etch-polished manner and the bulk and surface damage thresholds measured and correlated with absorption (cw CO_2 laser calorimeter), Auger, LEED and SEM data. The damage measurements were made with a TEM_{00} CO_2 TEA laser with a 0.6 μsec pulse length.

Key Words: Laser damage, KCl, 10.6 μm, RAP, etch-polishing, laser windows

1. Introduction

The present results represent a continuation of work on Hughes Research Laboratories (HRL) Reactive Atmosphere Processing (RAP) KCl reported by A. Braunstein et al. [1][1] at the 1973 Laser Damage Symposium. Conventional methods of polishing KCl (Linde A and methanol on a flannel lap) are known to produce scratched and smeared surfaces, which contribute considerably to the 10 6 μm absorption [2] and scattering. A method of surface finishing which removes the damaged layer has been developed with a resultant improvement in the 10.6 μm calorimetric absorption, scattering, and laser damage measurements. Other techniques used to characterize the HRL-grown and finished RAP KCl include Auger spectroscopy, LEED, and SEM. Bulk laser damage threshold measurements on HRL RAP KCl raise interesting theoretical questions as the predicted trend for the damage threshold of KCl relative to that of NaCl is reversed.

2. Sample Preparation

The procedure for producing HRL RAP KCl has been described elsewhere. [3] The crystals produced exhibit some low-angle grain boundaries, but can be considered single crystal for most purposes. Press forged samples were fabricated from boules with minimum visible internal scatter and were essentially veil free. Press forging was done at 250°C to a reduction of 50% in height at a rate of 0.05 in. per minute per in. of remaining length. Grain size in the resulting windows was 5 to 10 μm average diameter.

Windows polished by conventional polishing techniques are extremely environment sensitive. Surfaces fogged over a period of several minutes on damp days. It was therefore difficult to establish standards of measurement for KCl windows as the data changed with time. Figure 1 illustrates the microscopic difference between fogged and unfogged surfaces. It was also believed that the surface quality was setting a limit to the absorption and scattering measurements, effectively masking any improvement in bulk crystal quality that had been achieved.

J.W. Davisson [4] of Naval Research Labs had reported that concentrated HCl was a good etch for single crystal KCl. We have developed a modification of Davisson's procedure which consistently produces high quality surfaces. Conventionally polished KCl windows are agitated in concentrated HCl for 1 to 2 minutes (depending on the quality of the polished surface and the depth of the scratches), rinsed quickly in isopropyl alcohol, and then immersed in the vapor of a Freon TF degreaser to remove the alcohol and any remaining HCl.

*Work partially supported by Defense Advanced Research Projects Agency under the technical cognizance of Air Force Cambridge Research Laboratories.

[1]Figures in brackets indicate the literature references at the end of this paper.

Preceding page blank

3. Sample Characterization

Optical micrographs of a conventionally polished and etch-polished KCl window are shown in Figure 2. In contrast to the scratches and digs observed in the conventionally polished window, the etch-polished surface shows no discernible features at this magnification. This smoothness is confirmed hy SEM photographs at 18,000X (Figure 3).

Absorption coefficients measured calorimetrically at 10.6 μm for HRL RAP KCl, along with similar data for Optovac KCl for comparison, are giver in Table 1. The values quoted for the absorption coefficient are total absorption of the sample, including surface contributions. The range of values for the etch-polished HRL RAP KCl is much narrower than that shown by conventionally polished KCl and consistently lower.* This behavior is an indication of not only improved surface quality, but also improved stability of the surfaces. It is also now possible for us to distinguish bulk quality differences, which were not noticeable in conventionally polished windows. As an environmental test, a window cut from an early boule measured $\alpha = 0.00032$ cm^{-1} after etching. When measured after three weeks in a desk drawer, protected only from dust during a period of high humidity, $\alpha = 0.0004$ cm^{-1}, and window was not visibly fogged.

Table 1. 10.6 μm Absorption of KCl

	Absorption, cm^{-1}*
HRL RAP KCl	
Single Crystal	
Conventionally Polished	0.0008 to 0.0020 cm^{-1}
Etch Polished	0.00013 to 0.00020 cm^{-1}
Press Forged	
Conventionally Polished	0.00045 to 0.0021 cm^{-1}
Etch Polished	0.00022 to 0.00024 cm^{-1}
Optovac KCl	
Conventionally Polished	0.001 to 0.002 cm^{-1}
Etch Polished	0.0004 to 0.0014 cm^{-1}

*Total absorption of sample – includes bulk and surface.

*Preliminary experiments by us and others [5] indicate that the measured absorption coefficients in the 1 to 2 x 10^{-4} range might actually be instrument limited and represent upper limits to the actual absorption.

Auger analysis and LEED patterns [6] were recorded for four samples representative of different types of surface finishing: a cleaved Czochralski (Optovac) window, a similar cleaved window subjected to a 1 minute HCl etch as previously described, a polished HRL RAP window of unknown crystallographic orientation, and a polished blank from the same boule also etched for 1 minute; the results are given in Table 2. The initial Auger scans show the normal contaminants as all of the surfaces were prepared in air. Most of these trace contaminants are removed by 6 minutes of Ar^+ sputter cleaning. The residual oxygen can be ascribed to system contamination. The initial LEED patterns indicate some surface disorder in the cleaved Optovac sample and the etch-polished HRL RAP sample (B15-7), while the conventionally polished HRL RAP window (B15-8) displays essentially complete absence of surface order. The etched, cleaved Optovac window exhibited a great degree of surface order as shown by the appearance of first, second, and third order diffraction in the LEED pattern. A six minute Ar^+ sputter clean improved all of the LEED patterns with the exception of the conventionally polished sample (B15-8). An additional hour of Ar^+ sputter cleaning (removal of ~ 5 μm total) was necessary to obtain a diffuse LEED pattern for HRL B15-8. The data on the two samples of cleaved Optovac material (etched and unetched) indicate that a relatively thin layer (≤ 0.4 μm) of surface disorder is generated in the cleaving process, which is removed in the etch procedure. The residual diffusivity of the etch-polished HRL RAP window LEED pattern, can be at least partially attributed to the fact that the crystals were not cut along a symmetry axis. The resulting asymmetry of the LEED pattern makes it difficult to characterize. It is also quite possible that a longer etch time would have been necessary to remove all of the surface disorder caused by conventional polishing.

Table 2. Leed and Auger Data on Various KCl Samples

Sample	Initial		After 6.0 min Ar^+ Sputter-Clean (800 eV, 10 μA/cm^2)		After 1 Hour Ar^+ Sputter-Clean (800 eV, 10 μA/cm^2)	
	Leed Pattern	Auger Scan	Leed Pattern	Auger Scan	Leed Pattern	Auger Scan
1. Cleaved Optovac KCl	Diffuse	S, O, C	Sharp	O, C $O_f/O_i = 0.15$ $O_f \sim 1\%$		
2. Cleaved Optovac KCl Etched 1 min	Sharp (1st,2nd,3rd order)	O,C (Trace)	Sharp (Best)	O, I $O_f/O_i = 0.25$		
3. RAP B15-8 Polished	No	S, O, C (Trace)	No	O (Trace)	Weak, Diffuse	O (Trace)
4. RAP B15-7 Etched 1 min	Weak, Diffuse	S, O, C (Trace)	Sharper but still weak, diffuse	O (Trace)		

Relative total (surface and bulk) scattering at 10.6 μm was measured using a stabilized (0.1%) 200 mW cw CO_2 laser; these measurements are given in Table 3. The laser beam, focused to a 50 μm spot, was scanned across the sample and the scattering amplitude in the central portion of the scan was averaged and normalized to a similar measurement on conventionally polished HRL RAP KCl. As is indicated in the table, the lowest scattering is from etch polished, single crystal HRL RAP KCl. For the press forged material, etch polished windows show more scatter in the visible than conventionally polished blanks, but less at 10.6 μm as shown in Table 3. It is known that grain boundaries are preferentially etched in concentrated HCl and the enhanced grain boundaries contribute to the visible scatter, but do not affect the 10.6 μm scatter appreciably.

Table 3. Relative Scattering 10.6 μm

Single Crystal		
Mech Polished	KCl	1.0
Etched Polished	KCl	0.45
Press Forged		
Mech Polished	KCl	2.3
Etched Polished	KCl	0.72

4. Laser Damage Thresholds

The laser damage test facility, used to obtain the current results, is described in detail in another part of these proceedings. [7] Briefly, the laser is an ultraviolet preionized TEA laser operated in the TEM_{oo} mode, with 200 mJ maximum output energy. The equivalent rectangular pulse length is 0.6 μsec, but the actual pulse consists of many 2 nsec longitudinal mode spikes. Damage thresholds are reported in terms of the average power in the equivalent rectangular pulse. The actual peak power is approximately 5X the average power. Both a 5 in. focal length and 2.5 in. focal length lens were used in measuring the damage thresholds with measured beam waist spot sizes of 120 and 70 μm, respectively. The measured spot size of 70 μm for the short focal length lens is probably an upper limit. The actual spot size lies in a range from 60 μm (the calculated diffraction limited spot size) and the measured 70 μm. (cf Ref. 7.)

All tests were conducted in an evacuated sample chamber equipped with an x-y translation stage. Sites to be tested were selected with a 6X microscope to be free of cosmetic defects observable at that magnification; the onset of damage was monitored with the same microscope. In the samples for which high damage thresholds were measured, damage was so catastrophic that sophisticated observational techniques were unnecessary. For those sites where the apparent threshold at 6X magnification could not be reached, microscopic evaluation at 220X revealed no additional damage morphology. The range of damage thresholds reported represent the lowest power at which damage occurred to the highest power at which damage could not be effected.

The surface damage thresholds for polished KCl, reported in Table 4, are given mainly for historical perspective. All of the values reported are for the laser focused on the exit surface using the 5 in. focal length lens. The thresholds vary over quite a range, and do not correlate well with the absorption data. Since the absorption data were, of necessity, taken before the damage measurements, changes in the surface quality that occurred between the two measurements cannot be tracked easily.

Table 4. Surface Laser Damage Threshold Polished KCl

Sample	Absorption (cm^{-1})	Damage Threshold Energy Density (J/cm^2)	Damage Threshold Power Density (GW/cm^2)
Single Crystal			
RAP 824-6	0.00078	70-85	0.12-0.14
RAP 811-11	0.00070	> 110	> 0.18
RAP B53-4	0.0022	350	0.58
Optovac	0.024	18	0.03
Harshaw "Polytran"	0.0016	15	0.025

The character of the exit surface damage morphology for polished KCl is illustrated in Figure 4. The central portion of the damage site has been melted and is surrounded by a ring with a relatively smooth topography as compared to the undamaged portion of the surface. Radiating from this "cleaned" area are shallow cleavage planes. This type of shallow damage is observed only on poor surfaces and at relatively low damage thresholds in KCl.

In contrast to polished KCl the etched HRL RAP KCl absorption data do seem to correlate with the laser damage performance. The highest exit surface damage thresholds for etched HRL RAP KCl (Table 5) are measured on those samples with the lowest absorption and vice versa. Those samples marked by an asterisk were measured with the 2.5 in. focal length lens and the others with the 5 in. focal length lens. The wide range of values reported for sample RAP B53-1 is an exception to the convention for reporting thresholds. This particular sample at any one site either damaged, at a relatively low energy density (600 J/cm^2), or did no damage to the limit of the laser power output. The best (and most recent) etched HRL RAP KCl samples have a measured damage threshold for exit surface damage at least an order of magnitude greater than the threshold for conventionally polished KCl.

Table 5. Surface Laser Damage Threshold Etch KCl

Sample	Absorption (cm^{-1})	Damage Threshold Energy Density (J/cm^2)	Damage Threshold Power Density (GW/cm^2)
Single Crystal			
RAP B53-2	0.00026	380-520	0.63-0.87
RAP B53-4	0.00043	330-450	0.55-0.75
RAP B53-1	0.00020	600-2500+	1.0-4.2+
*RAP B63-2	0.00015	1500-2700	2.4-4.5
Harshaw Cleaved	———	60-135	0.10-0.22
Press Forged			
*RAP B37-17	0.00023	1500-1800	2.4-3.0
*RAP B37-16	0.00024	1650	2.7

Exit surface damage thresholds for press forged HRL RAP KCl are lower than those for single crystalline material, although not enough samples have been tested to date to establish this trend as definitive. The presence of "V grooves" in the form of preferentially etched grain boundaries in the polycrystalline KCl would, according to the theory of Bloembergen, [9] lead to lower damage thresholds due to enhanced dielectric breakdown.

Exit surface damage morphology for etched HRL RAP KCl differs markedly from that for polished surfaces (Figure 5). The damage sites are several millimeters in diameter and are composed of radiating cleavage planes. This type of behavior – minor damage at low thresholds for "dirty" surfaces, catastrophic damage at high thresholds for "clean" surfaces – had been noted by Giuliano [8] in measurements on ion-polished sapphire at 0.69 μm. The cleavage planes of exit surface damage sites in etched polycrystalline HRL RAP KCl (Figure 6) are distorted, compared to those in etched single crystal material, and seem to indicate the presence of grain boundaries. Inclusion damage, both bulk and surface, is readily distinguishable by damage morphology. A typical inclusion damage site (Optovac KCl, bulk damage) is illustrated in Figure 7. The damage region extended for a length of 400 μm along the beam path with many inclusion damage sites observable.

The bulk laser damage thresholds for HRL RAP KCl are given in Table 6, with measurements on one sample of Optovac KCl given for comparison. Because of the instability of the laser at low output powers, the bulk damage threshold of this particular sample of Optovac material could only be crudely bracketed. On the other extreme, the maximum available output power of the laser was not sufficient to damage one sample of single crystal and one sample of polycrystalline HRL RAP KCl. (In all fairness, it must be mentioned that other workers [10] have noticed a great variability in Optovac samples, and that we tested windows from only one sample.) For these measurements, the arguments for using the calculated diffraction limited spot size are particularly strong as the samples are thick enough (≈1 cm) that a

small error in measuring the focal distance and/or placement of the sample would still place the beam waist in the bulk of the material. Using the diffraction limited spot size would increase the damage thresholds by a factor of 1.4. Bulk damage in material with a high damage threshold has a very similar morphology to that exhibited by high damage threshold surface sites. Again the damage sites are massive and consist of radiating cleavage planes.

Table 6. Laser Damage Threshold Bulk KCl

Sample	Absorption (cm^{-1})	Damage Threshold Energy Density (J/cm^2)	Damage Threshold Power Density (GW/cm^2)
Single Crystal			
*RAP B53-1	0.00020	2500-3100	4.2-5.2
*RAP B63-2	0.00015	> 4600	> 7.8
*Optovac		> 180	> 0.3
		< 520	< 0.9
Press Forged			
*B37-15 (End)	Veiled	3700	6.3
*B37-15 (Center)	0.00064[+]	> 4600	> 7.8

[+]Conventionally polished sample, all others etch polished.

5. Dielectric Breakdown

The most generally accepted theory of laser induced breakdown in low absorption solids is that damage occurs via electron avalanche breakdown, and thus is a function of the peak electric field in the laser pulse. A recent paper by N. Bloembergen [11] reviews the subject of dielectric breakdown in solids, and summarizes the experimental evidence to date. [12,13,14] The data of E. Yablonovitch [12] at 10.6 μm and Von Hippel [14] (dc measurements) are given in Table 7, along with the HRL data. The electric field strength and power densities were calculated and measured slightly differently in the Yablonovitch and HRL data. Yablonovitch used peak power measurements (≈ 2X average) [12] and the diffraction limited spot size in calculating the breakdown electric fields. The HRL measurements are calculated using the average power and a measured spot size. For comparison, the HRL breakdown thresholds calculated using the diffraction limited spot size are given in parentheses in Table 7. In order to eliminate the differences in experimental conditions between the Yablonovitch and HRL data, the KCl data was normalized to Harshaw NaCl. According to Yablonovitch, [15] commercial NaCl yields damage thresholds consistent from sample to sample and thus we used it as a standard. The theoretical prediction from periodic table trends was that NaCl should have a damage threshold at 10.6 μm greater than that exhibited by KCl. In data given by Yablonovitch, this trend holds true for samples of comparable purity for both compounds. The HRL RAP KCl, on the other hand, has a considerably higher damage threshold than Harshaw NaCl, effectively reversing the trend for KCl/NaCl. This data is seen to lend support to the hypothesis of Hellwarth [16] that electron avalanche breakdown is impurity mediated, i.e., the observation of dielectric breakdown does not necessarily indicate that the ultimate limit for damage has been reached for a given material. It is expected that damage thresholds on HRL RAP NaCl (presumed to be comparable to HRL RAP KCl in purity) would be higher than those measured on Harshaw NaCl, and would, perhaps restore the expected relationship: breakdown (NaCl) > breakdown (KCl).

6. Conclusions

We have developed a technique for generating high quality, relatively undamaged surfaces on HRL RAP KCl. The improvement in surface quality enables us to better evaluate bulk quality, and various characterizing measurements have been developed to judge surface and bulk quality. The results of these measurements seem to correlate qualitatively with the measured damage thresholds. The damage threshold of the surface has improved by at least an order of magnitude and approaches the bulk damage threshold in some samples.

The measurements of bulk damage threshold support the theory that sample purity affects the "intrinsic" electron avalanche breakdown damage threshold.

Table 7. Comparison of Laser Damage KCl and NaCl

	Yablonovitch (1972)		HRL (1974)*		Von Hippel (1937)	
	KCl	NaCl	KCl	NaCl	KCl	NaCl
Power (GW/cm^2)	3.7	7.5	>7.8(10.6)	4.8(6.5)		
	KCl/NaCL = 0.49		KCl/NaCl = 1.6			
Electric Field (MV/cm)	1.39	1.95	>2.0(2.4)	1.6(1.9)	1.0	1.5

*Parenthetical values were calculated using the diffraction limited spot size (60 μm) instead of the measured 70 μm.

7. Acknowledgments

The authors gratefully acknowledge the help and assistance of Roger Turk, Bernie Garcia, Paul Coker, and Oon Williams. The many technical discussions with Art Braunstein were invaluable. The efforts of the HRL optical polishing shop, George Heussner and Matt Himber, are also appreciated.

8. References

[1] Braunstein, A.I., Wang, V., Braunstein, M., Rudisill, J.E., and Wada, J. NBS Special Publication Laser Induced Damage in Optical Materials, A.J. Glass and A.H. Guenther, Ed., 1973, p. 151.

[2] Braunstein, M. "Laser Window Surface Finishing and Coating Technology," ARPA Contract F19628-73-C-0243.

[3] Pastor, R.C., and Braunstein, M., "Advanced Mode Control and High Power Optics Technology," Tech. Report, AFWL-TR-72-152, Vol II.

[4] Oavisson, J.W., Conference on High Power IR Laser Windows, Vol. 2, November 1972, p. 525-534.

[5] Haas, M., Naval Research Labs, private communication.

[6] Physical Electronics Industries, Inc., Edina Minn., Model #10-234G.

[7] Wang, V., et al., these proceedings.

[8] Giuliano, C., Appl. Phys. Lett., 21, 39 (1972).

[9] Bloembergen, N., Appl. Opt., 12, 661-664, 1973.

[10] Bernal G. E., Honeywell, private communication.

[11] Bloembergen, N., IEEE J. of Quantum Electron., QE-10, 375-386, 1974.

[12] Yablonovitch, E., Appl. Phys. Lett., 19, 495-497, 1971.

[13] Fradin, D.W. and Bass, M., Appl. Phys. Lett., 22, 206-208, 1973.

[14] Von Hippel, A., J. Appl. Phys., 8, 815-832, 1937, Phys. Rev. 54, 1096-1102, 1938.

[15] Yablonovitch, E., private communication.

[16] Hellwarth, R.W., NBS Special Publication, Damage in Laser Materials, A.J. Glass and A.H. Guenther, Ed., 1970, p. 67.

List of Figures

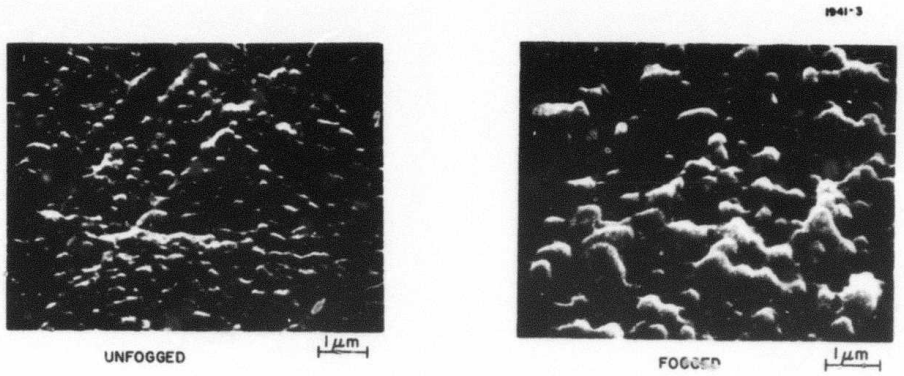
1941-3
UNFOGGED
1 μm
FOGGED
1 μm

Fig 1.

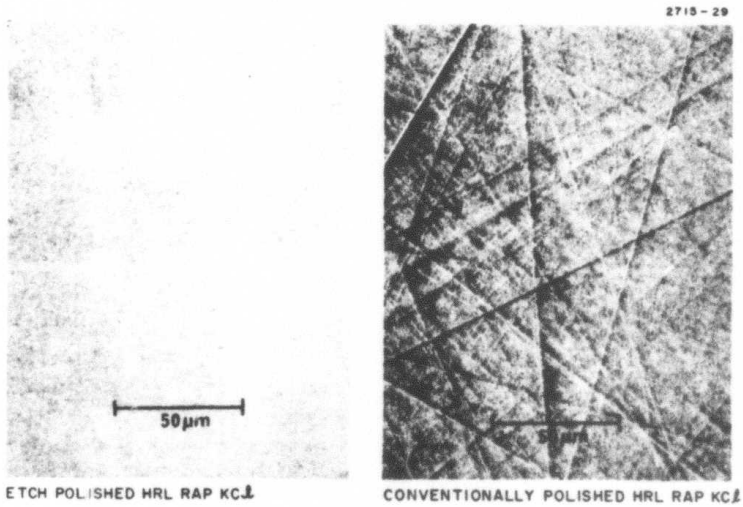
2715-29
50 μm
ETCH POLISHED HRL RAP KCl
CONVENTIONALLY POLISHED HRL RAP KCl

Fig. 2.

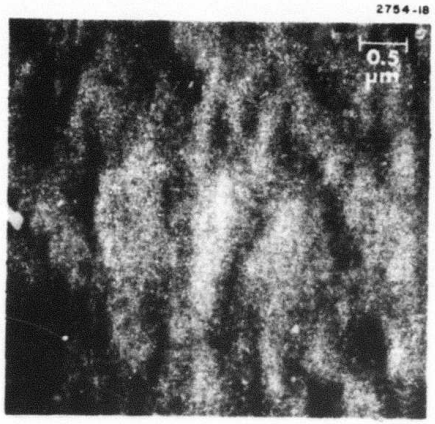

BEAM ≈ 70° TO SURFACE

Fig. 3

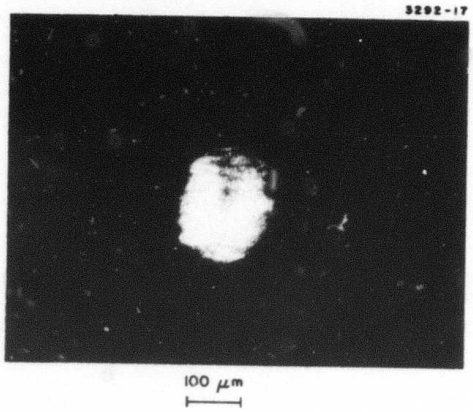

Fig. 4

Fig. 5

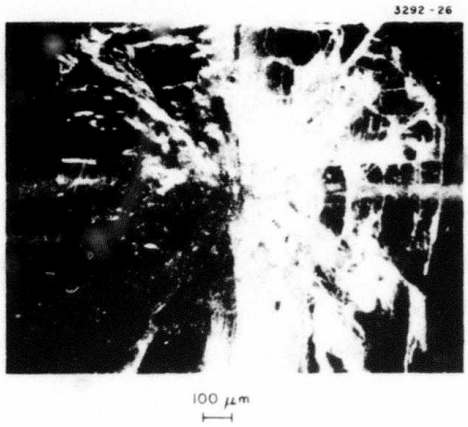

Fig. 6

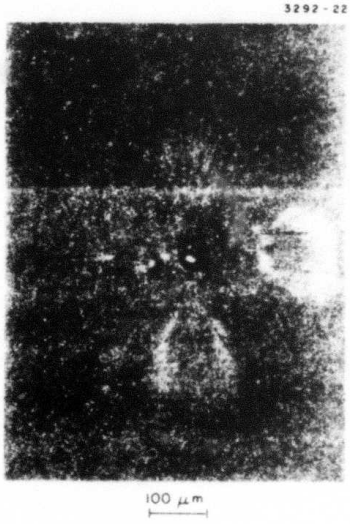

Fig. 7

PULSED CO_2 LASER DAMAGE IN WINDOWS, REFLECTORS, AND COATINGS

V. Wang, J.E. Rudisill, C.R. Giuliano, M. Braunstein, and A. Braunstein

Hughes Research Laboratories
3011 Malibu Canyon Road
Malibu, California 90265

Presented at the Symposium on Damage in Laser Materials, Boulder, Colorado, May 1974. To be published in the Proceedings.

Preceding page blank

Pulsed CO_2 Laser Damage in Windows, Reflectors, and Coatings*

V. Wang, J.E. Rudisill, C.R. Giuliano, M. Braunstein, and A. Braunstein

Hughes Research Laboratories
3011 Malibu Canyon Road
Malibu, California 90265

Recent 10.6 μm damage measurements using a TEM_{00} laser of 0.6 μsec pulse length are reported for a variety of windows, reflectors, and coatings. Reduction of the density of inclusions in ZnSe was found to have a large effect upon scatter but a smaller effect upon damage resistance. Absorptions and damage thresholds of thin films of ZnSe, As_2S_3 and ThF_4 were measured upon relatively defect-free KCl substrates, and then tested in antireflection and multilayer reflector configurations. Also reported is a five-fold increase in damage resistance of simple polished copper reflectors by surface etching.

Key Words: As_2S_3, laser coatings, laser reflectors, laser windows, pulsed CO_2 laser damage, ThF_4, and ZnSe.

1. Introdution

Since 1971 we have been involved in the development of damage resistant, low absorption, optical components at 10.6 μm.[1,2][1] Since our prior experiments have indicated that wide bandgap materials are as damage resistant as simple polished metal reflectors and that semiconductor materials are considerably less damage resistant, this paper reports upon recent development of three wide bandgap materials: ZnSe, As_2S_3, and ThF_4. These results are compared with recent progress in metal reflectors.

2. Experimental Conditions

An ultraviolet CO_2 TEA laser discharge 50 cm in length, operating at 550 Torr with 1:1:8 mixture of CO_2:N_2:He was used in this experiment. A two-meter, approximately hemiconfocal cavity operating in the TEM_{00} mode with an uncoated germanium resonant output reflector delivers an essentially untruncated gaussian beam to a folded optical train (illustrated in Figure 1). A beam attenuator consisting of two wire grid polarizers on ZnSe substrates allows better than two orders of magnitude attenuation without rotation of the output polarization.[3] Wedged NaCl beamsplitters allow monitoring of the energy in each pulse by a polyvinylchloride (PVF) pyroelectric detector. Absolute calibration of the pyroelectric monitor is provided by a Hadron Model 100 cone thermopile with a 1 cm aperture located in the near field of the laser.

The output pulse of the laser consists of a 200 nsec gain-switched pulse followed by a nitrogen fed tail of ∿3 μsec. Figure 2(a) displays the output detected by a germanium photon drag detector, and Figure 2(b) is an expanded trace showing a typical example of the partially self-mode locked beating in the output. Power density is measured at the peak of the gain switched spike by using a detector that averages the rapid pulsations from mode beating, as shown in Figure 2(c). An equivalent pulse length is defined by measuring the area of Figure 2(c) and constructing an equivalent rectangular pulse of equal area and height equal to the height in Figure 2(c).

---

*Work partially supported by Air Force Weapons Laboratory, Kirtland Air Force Base and by Defense Advanced Research Projects Agency under the technical cognizance of Air Force Cambridge Research Laboratories.

[1]Figures in brackets indicate the literature references at the end of this paper.

For thermal damage mechanisms, the effect of nanosecond pulses is negligible with respect to the total pulse energy, so total pulse energy and pulse length closely characterize the pulse. For electrical breakdown mechanisms in inclusion-free dielectrics, simple considerations predict a pulse length dependence for the electric breakdown field due to the finite time required to form sufficient electrons through avalanche. Our extrapolation of calculations by Yablonovitch and Bloembergen [4] suggests that a pulse 2 nsec long would be expected to have a breakdown threshold 4 to 8 times higher in power density than a 0.2 μsec pulse. From Figure 2(c), the peak intensity of this pulse is approximately 5 times the average intensity, so it is the average power in the gain switched pulse that is reported in both this paper and the paper by S.O. Allen, et al., [7] on surface and bulk damage in KCl.

Spot size for a given lens is measured by varying the energy focused on a heat-sensitive plastic film (3 M, Type 557) in a series of burn spots, and plotting the log of energy versus spot size squared (Figure 3). A pulse of gaussian profile yields a straight line whose slope is a measure of the spot size. Measurements of spot size using the 12.5 cm germanium lens used for the majority of the tests indicate an essentially diffraction-limited spot size to beyond the $1/e^2$ intensity points. Measurements of spot size at the focus of the 6.2 cm lens give a diameter of between 0.059 mm and 0.073 mm (Figure 3). The uncertainty in measurement for this lens is due in part to the difficulty of measuring the low energies used in this calibration. Energy densities quoted for this lens are calculated for the on-axis peak intensity of a 0.073 mm spot. If a diffraction-limited waiste is assumed, energy and power densities would be 50% higher for this lens at the beam waist.

Both windows and reflectors are tested in a sample chamber evacuated below 1 Torr to eliminate spurious effects caused by dust and air breakdown induced near the surface of a sample. Damage threshold in this paper is defined as the first visible, permanent change in the appearance of the sample viewed at high magnification in an optical microscope, unless otherwise stated. During the tests the sample is observed at ∿10x.

3. Test Results

Zinc selenide has been of major interest as a high power window material. Previous results [2,5,6] have indicated that inclusions that visibly lie in bands within the material limit the damage threshold, as shown in Figure 4. In an effort to explore the effects of improved materials process control, regions of low scatter were selected for damage testing. The ZnSe surfaces were etch polished with potassium ferricynide on both the samples in Tables 1 and 2 to remove a damaged surface layer. Scattering measurements at 10.6 μm show a tenfold reduction in scatter for the selected clear areas. However, the damage threshold, reported in Table 1, shows only a small improvement in damage resistance.

Table 1. Measured Thresholds of Damage in ZnSe Windows

Material	Absorption cm^{-1}	Relative Scatter, 10.6 μm	Damage Threshold		Comments
			Energy Density, J/cm^2	Power Density,[a] MW/cm^2	
Banded region, R-26	0.0030	1	30 to 40	50 to 70	Inclusion damage
Unbanded region, R-26	0.0021	0.1	55	90	Inclusion damage or localized surface absorption sites

[a]Based on τ = 0.6 μsec.

Wide bandgap high and low index materials are useful for antireflection coating on windows and multilayer dielectric reflectors. Zinc selenide (n = 2.41) and As_2S_3 (n = 2.38) are promising materials for high index films and ThF_4 (n = 1.35) is the only nonhydroscopic material available of low index and low absorption at 10 μm. In order to evaluate the performance of individual films, λ/4 wave layers have been deposited on relatively defect-free surfaces of low absorption etch-polished RAP grown KCl. [7] These substrates allow accurate calorimetric absorption measurements to be made and also provide a damage-resistant substrate.

Table 2. Measured Damage Thresholds in Thin Films and AR Coatings

Coating and Substrate	Absorption	Measured Damage Threshold		Comments
		Energy Density J/cm^2	Power Density[a] MW/cm^2	
$\lambda/4$ ThF_4 on KCl	10 cm^{-1}	80 J/cm^2	130	
$\lambda/4$ As_2S_3 on KCl	<1 cm^{-1}	120 J/cm^2	200	
$\lambda/4$ ZnSe on KCl	<0.6 cm^{-1}	140 J/cm^2	230	Poor adhesion of film
ZnSe/ThF_4 AR on KCl	0.2% per surface	60	100	
ThF_4/ZnSe AR on ZnSe	N.A.	25 to 40 J/cm^2	40 to 70	Limited by substrate
ThF_4/ZnS AR on ZnSe	N.A.	30 to 40 J/cm^2	50 to 70	Limited by substrate

[a]Based on τ = 0.6 μsec.

To compare the values given in Table 2 for ZnSe films with the bulk values in Table 1, we can calculate the electric field distribution in the film as shown in Figure 5. Assuming a plane wave entering from the left, Figure 5 plots the normalized electric field versus depth into the $\lambda/4$ film in micrometers. The average electric field in the layer is within a few percent of the field in a bulk ZnSe window. The film has an absorption coefficient of approximately 0.1 cm^{-1}, while bulk ZnSe has an absorption coefficient of 0.002 to 0.003 cm^{-1} (assuming the absorption is uniformly distributed), the film has a coefficient of approximately 0.1 cm^{-1}. In this case the absorbed energy density in the film would be 30 to 50 times larger than that in the bulk samples, and its damage threshold would be expected to be correspondingly lower. Thus, the higher damage threshold observed in the film may be a result of the relative lack of absorbing inclusions. In the case of ThF_4, as a result of the relatively high absorption coefficient, linear absorption alone can account for a temperature rise to near the melting point. The performance of ThF_4, ZnSe, and ZnS coatings in an antireflection design on ZnSe substrates is shown in the bottom half of Table 2. As expected, the incident flux is limited by damage due to substrate inclusions near the surface.

The performance of some of these films in reflector designs is summarized in Table 3. Apparently because of localized absorbing centers, visible plasmas form near the surface at a low energy density, but gradual power increase removes these artifacts without damage to the overall integrity of the films. Since visible scattering remains relatively high in these preliminary samples, it might be expected that considerable improvement is possible. The last sample in Table 3, a $(ThF_4/ZnSe)^2$ reflector on an electroless nickel substrate, exhibits a reproducible improvement by a factor of more than 4 over the several sites tested on its surface, without any intentional changes in the film deposition techniques. However, the scatter of this sample was lower than the previous ones. Figure 6 is an exact computer calculation of the electric field distribution within this dielectric reflector, including the effects of absorption. As can be seen, the peak electric field within the reflector occurs at the outermost interface between the high and low index films, and is approximately 20% higher than the $\lambda/4$ film on KCl. The field approaches zero on the outer surface of the stack and is also small at the metal substrate boundary. The substrate absorbs about 0.07% of the incident flux, or 32% of the total absorption of the reflector.

Whereas simple uncoated metal reflectors have proved to be among the most damage-resistant optical components examined, recent results have indicated an improvement of 3 to 4 in damage resistance by superpolishing of dispersion-hardened copper mirrors. [8] However, this improvement was not observed in superpolished molybdenum. In an effort to isolate the mechanism responsible for the improvement, samples of OFHC copper were polished and etched by metallographic techniques designed to remove all surface contaminents from abrasives, and to leave an unworked surface highlighting the grain structure. This surface is not an acceptable mirror in the visible due to high scatter, but exhibits a marked increase in damage resistance, similar to that seen in superpolished materials. Table 4 summarizes this development, and compares the results with a conventionally polished sample. Etch-polishing techniques to yield a smoother surface of low scatter are presently under consideration. It is necessary to qualify the applicability of these numbers to large-scale beams. Because of the small beam sizes incident upon some of the samples (120 μm), three-dimensional heat diffusion can be expected to cool the surface at a greater rate than one-dimensional heat diffusion, as experienced in large-scale beams. Large-scale beams would thus be expected to exhibit a lower damage threshold.

Table 3. Measured Thresholds of Damage in ThF_4/ZnSe Multilayer Reflectors

Substrate	Coating	Absorption, %	Measured Damage Threshold		Comments
			Energy Density, J/cm^2	Power Density[a] MW/cm^2	
Mo	$(ThF_4/ZnSe)^2$	0.22	50	80	Conditions with gradual power increase
Mo	$(ThF_4/ZnSe)^3$	0.32	30	80	Conditions obvious scattering sites
Al/E-Ni	$Ag/(ThF_4/ZnSe)^2$	0.2	270	450	Scattering sites visible

[a]Based on τ = 0.6 μsec.

Table 4. Measured Thresholds of Damage in Metal Reflectors

Coating and Substrate	Damage Threshold		Comments
	Energy Density J/cm^2	Power Density[a] MW/cm^2	
Cu, conventional polish	90 150	150 250	25.4 cm focusing lens used 12.7 cm focusing lens used
Mo, sputtered Mo coating	4 to 8	7 to 13	25.4 cm focusing lens used
OFHC Cu, polish and etch	750	1200	No imbedded abrasive unworked surface High visible scatter 12.7 cm focusing lens used

[a]Based on τ = 0.6 μsec.

4. Summary

By careful measurement of spot sizes and temporal profile, we have attempted to precisely define the on-axis energy and power. Results of tests upon thin films currently indicate that wide bandgap materials are capable of damage thresholds comparable to metal reflectors, and that simple linear absorption can be the limiting factor rather than inclusion damage.

It has been further concluded that inclusions or surface contamination play an important role in limiting the damage resistance of copper mirrors. Improvements in surface preparation have improved damage resistance by better than a factor of four.

5. Acknowledgments

We wish to thank Roger Turk for his invaluable expertise in microscopy and in the metallographic preparation of the copper reflectors, Bernardo Garcia and John Bowers for the preparation of dielectric films, and Tomas Horne for aid in the construction of the experiments.

6. References

[1] Wang, V., Braunstein, A.I., Braunstein, M., and Wada, J.Y., "Investigation of Pulsed CO_2 Laser Damage of Metal and Dielectric-Coated Mirrors," NBS Special Publication 372, Laser Induced Damage in Optical Materials (1972).

[2] Wang, V., Braunstein, A.I., Braunstein, M., Rudisill, J.E., and Wada, J.Y., "Pulsed CO_2 Laser Damage Studies of Metal and Dielectric Coated Mirrors," NBS Special Publication 3B7, Laser Induced Damage in Optical Materials (1973); and Braunstein, A.I., Wang, V., Braunstein, M., Rudisill, J.E., and Wada, J.Y., "Pulsed CO_2 Laser Damage Studies of Windows and Window Coatings," NBS Special Publication 387, Laser Induced Damage in Optical Materials (1973).

[3] Garvin, H.L., Kiefer, J.E., and Somekh, S., "Wire-Grid Polarizers for 10.6 μm Radiation," 1973 IEEE/OSA Conference on Laser Engineering and Applications.

[4] Yablonovitch, E., and Bloembergen, N., "Avalanche Ionization and the Limiting Diameter of Filaments Induced by Light Pulses in Transparent Media," Phys. Rev. Lett. 29, 14, 2 October 1972.

[5] Fradin, D.W., and Bua, D.P., "Laser-Induced Damage in ZnSe," Appl. Phys. Lett. 24, 11, 1 June 1974.

[6] Braunstein, M., "Laser Window Surface Finishing and Coating Technology," Third Conference on High Power Infrared Laser Window Materials, November 12-14, 1973.

[7] Allen, S.D., Braunstein, M., Giuliano, C., and Wang, V., "Pulsed CO_2 Laser Damage Studies of RAP Grown KCl, this Proceedings.

[B] Soileau, M.J., and Wang, V., "Improved Damage Thresholds for Metal Mirrors," Appl. Opt. 13, 6, June 1974.

FIGURE CAPTIONS

Fig. 1. Schematic of laser, optical train, and sample chamber.

Fig. 2. Pulse temporal profile. (a) Germanium photon drag detector plus 500 MHz oscilloscope. (b) Expanded to 10 nsec/division. (c) Definition of equilavent pulse (pyroelectric detector).

Fig. 3. Beam spatial profile and spot size.

Fig. 4. Zinc selenide cross section.

Fig. 5. Computed electric field in $\lambda/4$ ZnSe on KCl.

Fig. 6. Electric field distribution on a $Mo/(ThF_4/ZnSe)^2$ reflector.

3269-2

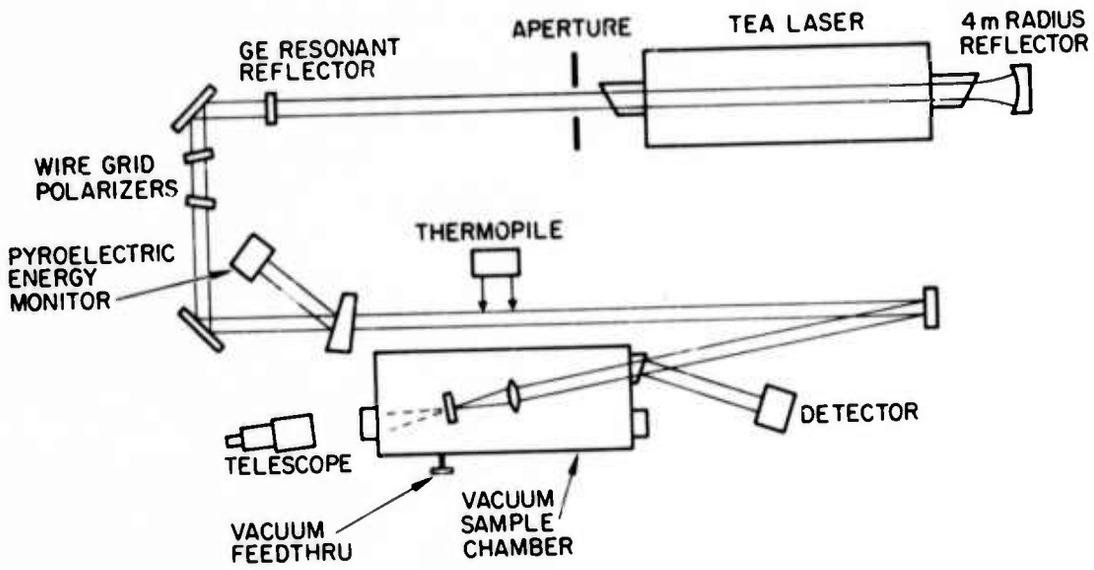

Fig. 1

EXPERIMENTAL PARAMETERS

LASER:

ENERGY - 200 MJ TEM_{00}, DIFFRACTION LIMITED

PULSE LENGTH (EQUIVALENT PULSE LENGTH) - 0.6 μSEC

BEAM DIAMETER AT OUTPUT (1/E ELECTRIC FIELD) - 0.5 CM

SPOT SIZES (1/E INTENSITY IN DIAMETER)

25.4 CM f.l. - 0.240 MM
12.7 CM f.l. - 0.120 MM
6.3 CM f.l. - 0.059 - 0.073 MM (EXP. UNCERTAINTY)

ATTENUATOR - WIRE GRID POLARIZERS

SAMPLE CHAMBER - EVACUATED TO <1 TORR

DIAGNOSTICS - VISUAL AT ~10X MAGNIFICATION

DETECTORS - HAORON MODEL 100 THERMOPILE, GE PHOTON DRAG DETECTOR, PYROELECTRIC DETECTORS

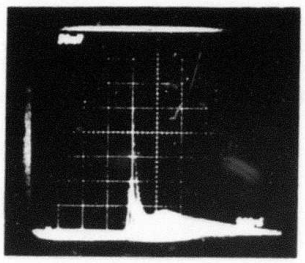

Fig. 2(a)

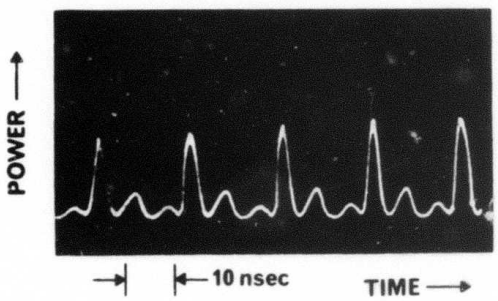

Fig. 2(b)

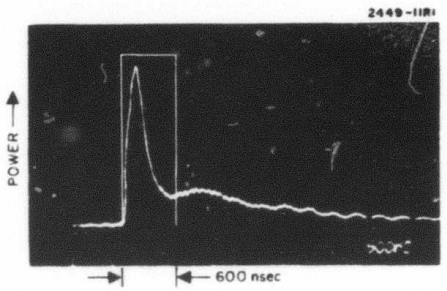

Fig. 2(c)

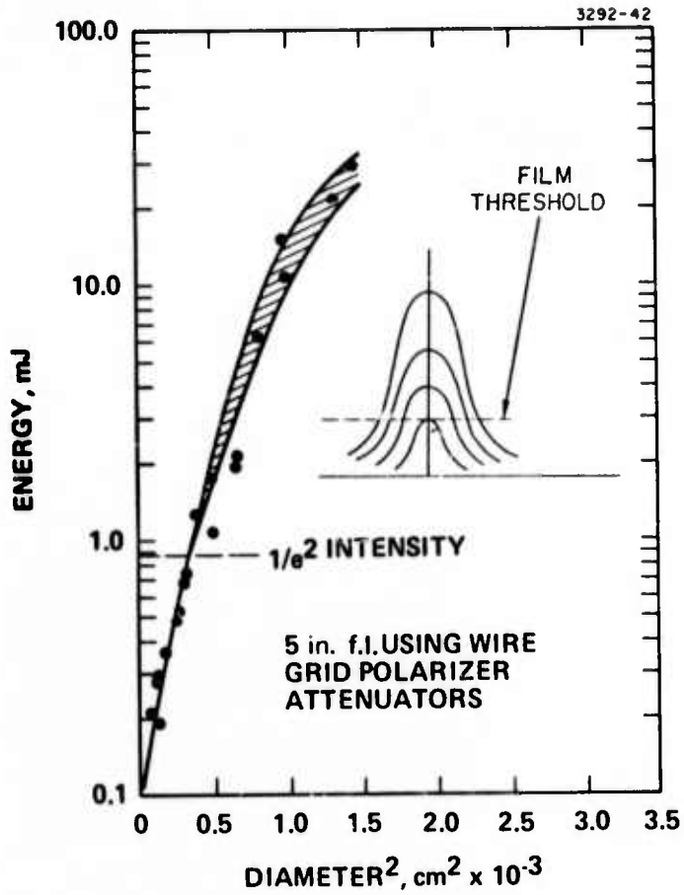

Fig. 3.

NOTE: BANDING (TOP DARK REGION). THIS COINCIDES WITH FACE WHICH POLISHED POORLY. BOTTOM EDGE COINCIDES WITH FACE GIVING EXCELLENT POLISH.

Fig. 4

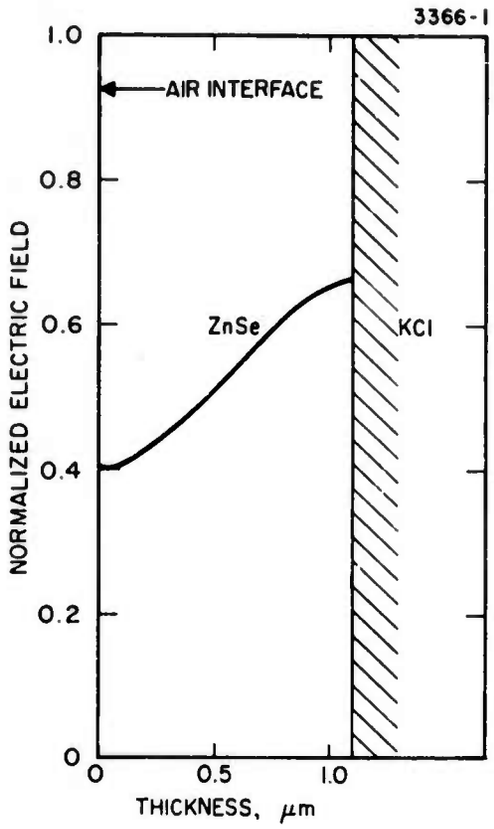
3366-1
1.0
0.8
0.6
0.4
0.2
0
AIR INTERFACE
ZnSe
KCl
NORMALIZED ELECTRIC FIELD
0
0.5
1.0
THICKNESS, μm

Fig. 5

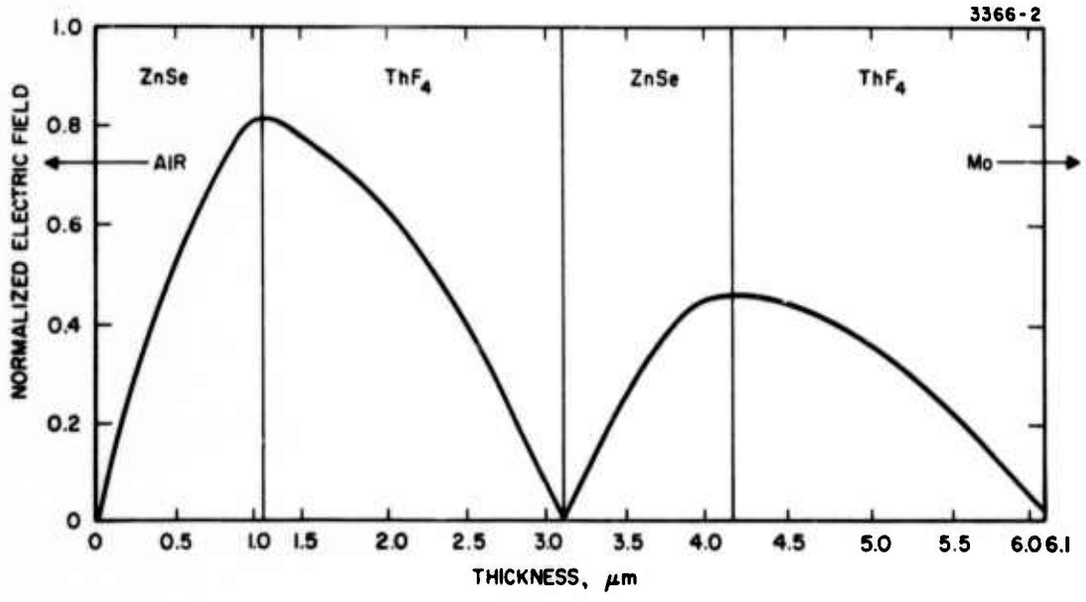
3366-2
1.0
0.8
0.6
0.4
0.2
0
ZnSe
ThF4
ZnSe
ThF4
AIR
Mo
NORMALIZED ELECTRIC FIELD
0
0.5
1.0
1.5
2.0
2.5
3.0
3.5
4.0
4.5
5.0
5.5
6.0
6.1
THICKNESS, μm

Fig. 6